
Laser-Induced Plasmas and Applications

edited by

Leon J. Radziemski

Department of Physics
New Mexico State University
Las Cruces, New Mexico

David A. Cremers

Chemical and Laser Sciences Division
Los Alamos National Laboratory
Los Alamos, New Mexico

MARCEL DEKKER, INC.

New York and Basel

Library of Congress Cataloging-in-Publication Data

Laser-induced plasmas : physical, chemical, and biological applications / edited
by Leon J. Radziemski, David A. Cremers.

p. cm.

Includes bibliographies.

ISBN 0-8247-8078-7 (alk. paper)

1. Plasma engineering. 2. High power lasers. I. Radziemski, Leon J.,
II. Cremers, David A.

TA2020.L37 1989

620.044--dc20

89-7883

CIP

This book is printed on acid-free paper.

Copyright © 1989 MARCEL DEKKER, INC. All Rights Reserved

Neither this book nor any part may be reproduced or transmitted in any form
or by any means, electronic or mechanical, including photocopying, microfilming,
and recording, or by any information storage and retrieval system, without per-
mission in writing from the publisher.

MARCEL DEKKER, INC.

270 Madison Avenue, New York, New York 10016

Current printing (last digit):

10 9 8 7 6 5 4 3 2 1

PRINTED IN THE UNITED STATES OF AMERICA

Contents

Preface	iii
Contributors	xi
1 Physics of Laser-Induced Breakdown: An Update	1
Guy M. Weyl	
1.1 Introduction	1
1.2 Creation of Initial Electrons	3
1.3 Electron Growth in Gases	8
1.4 Laser-Induced Breakdown of Solids and Liquids	36
1.5 Concluding Remarks	58
References	59
2 Modeling of Post-Breakdown Phenomena	69
Robert G. Root	
2.1 Introduction	69
2.2 Creation of a Propagating Plasma	70
2.3 Absorption Characteristics of Heated Gases	72
2.4 Features of Propagating Plasmas	75
2.5 One-Dimensional Laser-Supported Combustion Waves	77
2.6 One-Dimensional Laser-Supported Detonation Wave	88
2.7 One-Dimensional Laser-Supported Radiation Wave	92
2.8 Transition Regions	93
2.9 Radial Expansion	95
2.10 Thermal Coupling	99
2.11 Other Factors	100
2.12 Summary	101
References	101
3 Introduction to Laser Plasma Diagnostics	105
Allan A. Hauer and Hector A. Baldis	
3.1 Introduction	105
3.2 Introduction to Optical Diagnostics	110

x	Contents	
3.3	Introduction to X-ray Diagnostics	131
	References	161
4	Laser-Sustained Plasmas	169
	Dennis R. Keefer	
4.1	Introduction	169
4.2	Principles of Operation	172
4.3	Analytical Models	182
4.4	Experimental Studies	189
4.5	Applications of the Laser-Sustained Plasma	196
	References	203
5	Inertially Confined Fusion	207
	Robert L. McCrory and John M. Soures	
5.1	Historical Overview	207
5.2	Laser-Fusion Scaling Laws	211
5.3	Coronal Physics	217
5.4	X-ray Generation by Laser-Produced Plasmas	224
5.5	Laser-Driven Ablation	227
5.6	Hydrodynamic Stability of Ablatively Driven Shells	239
5.7	Irradiation Uniformity Requirements	243
5.8	Implosion Experiments	251
	References	260
6	Laser-Based Semiconductor Fabrication	269
	Joseph R. Wachter	
6.1	Aspects of Semiconductor Fabrication	269
6.2	Applications of Lasers in the Semiconductor Industry	276
6.3	Research Areas	283
6.4	Outlook	290
	References	291
7	Spectrochemical Analysis Using Laser Plasma Excitation	295
	Leon J. Radziemski and David A. Cremers	
7.1	Review	295
7.2	Methods and Properties of Analysis Using Laser Plasmas	296
7.3	Analysis of Gases	302
7.4	Analysis of Bulk Liquids	306
7.5	Analysis of Particles	309
7.6	Analysis of Solids	313
7.7	Advances in Instrumentation	318

Contents	xi
7.8 Prognosis	321
References	323
8 Fundamentals of Analysis of Solids by Laser-Produced Plasmas	327
Yong W. Kim	
8.1 Chapter Organization	327
8.2 Introduction	327
8.3 Phenomenology of Laser Heating of Condensed-Phase Targets	330
8.4 Quantitative Spectroscopy	336
8.5 Intensity Measurements and Elemental Analysis	341
8.6 Summary	344
References	345
9 Laser Vaporization for Sample Introduction in Atomic and Mass Spectroscopy	347
Joseph Sneddon, Peter G. Mitchell, and Nicholas S. Nogar	
9.1 Conventional Solid Sample Introduction for Atomic Spectroscopy	347
9.2 Laser Ablation of Solid Samples	350
9.3 Laser Ablation for Sample Introduction in Atomic Spectroscopy	353
9.4 Relative Merits of Laser Ablation for Sample Introduction in Atomic Spectroscopy	363
9.5 Laser Sources for Mass Spectrometry	365
9.6 Applications of Laser Microprobe	369
9.7 Applications of Laser Desorption and Postionization	372
9.8 Conclusion	376
References	376
10 Current New Applications of Laser Plasmas	385
Allan A. Hauer, David W. Forstund, Colin J. McKinstrie, Justin S. Wark, Philip J. Hargis, Jr., Roy A. Hamil, and Joseph M. Kindel	
10.1 Introduction	385
10.2 Applications of Laser-Plasma-Generated X-rays and Particles	386
10.3 Laser-Plasma Acceleration of Particles	413

10.4 Laser-Pulsed Power Switching	424
References	432
Index	437

4

Laser-Sustained Plasmas

Dennis R. Keefer
Center for Laser Applications
University of Tennessee Space Institute
Tullahoma, Tennessee

4.1 INTRODUCTION

Plasmas created by the radiation from focused laser beams were first observed with the advent of "giant pulse" Q-switched, ruby lasers by Maker et al. (1963). These plasmas formed spontaneously by gas breakdown at the focus of a lens and were sustained only for the duration of the laser pulse. Plasmas were also observed to form on the surfaces of materials irradiated by high-power pulsed or continuous lasers and to propagate into the incident beam at subsonic or supersonic velocities. With the advent of continuous, high-power carbon dioxide lasers, it became possible to sustain a plasma in a steady-state condition near the focus of a laser beam, and the first experimental observation of a "continuous optical discharge" was reported by Generalov et al. (1970). The continuous, laser-sustained plasma (LSP) is often referred to as a continuous optical discharge (COD) and it has a number of unique properties that make it an interesting candidate for a variety of applications.

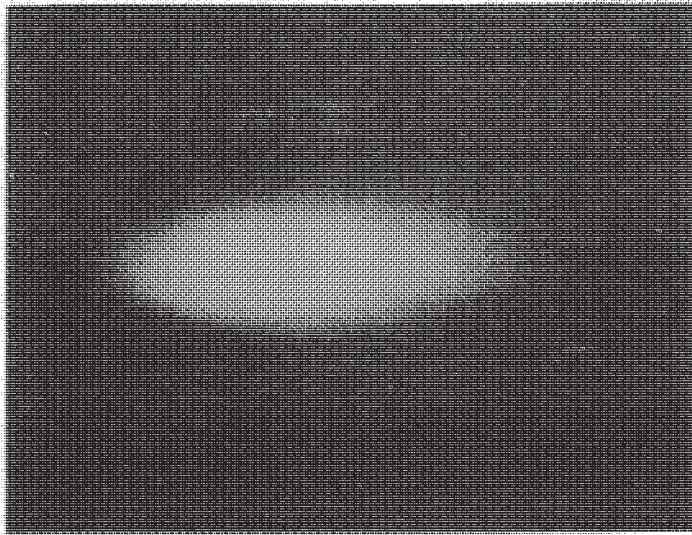
The laser-sustained plasma shares many characteristics with other gas discharges, as explained in detail by Raizer (1980) in his comprehensive review, but it is sustained through absorption of power from an optical beam by the process of inverse bremsstrahlung. Since the optical frequency of the sustaining beam is greater than the plasma frequency, the beam is capable of propagating well into the interior of the plasma where it is absorbed at high intensity near the focus. This is in contrast to plasmas sustained by high-frequency electrical fields (microwave and electrodeless discharges) that operate at frequencies below the plasma frequency and sustain the plasma through absorption within a thin layer near the plasma surface. This fundamental difference in the power absorption mechanism makes it possible to

generate steady-state plasmas having maximum temperatures of 10,000K or more in a small volume near the focus of a lens, far away from any confining structure. A photo of a plasma sustained by a laser beam focused with a lens is shown in Fig. 4.1(a). The 600 W Gaussian beam from a carbon dioxide laser was focused by a 191 mm focal length lens into 2 atm of flowing argon. Fig. 4.1(b) shows schematically how the plasma forms within the focal region.

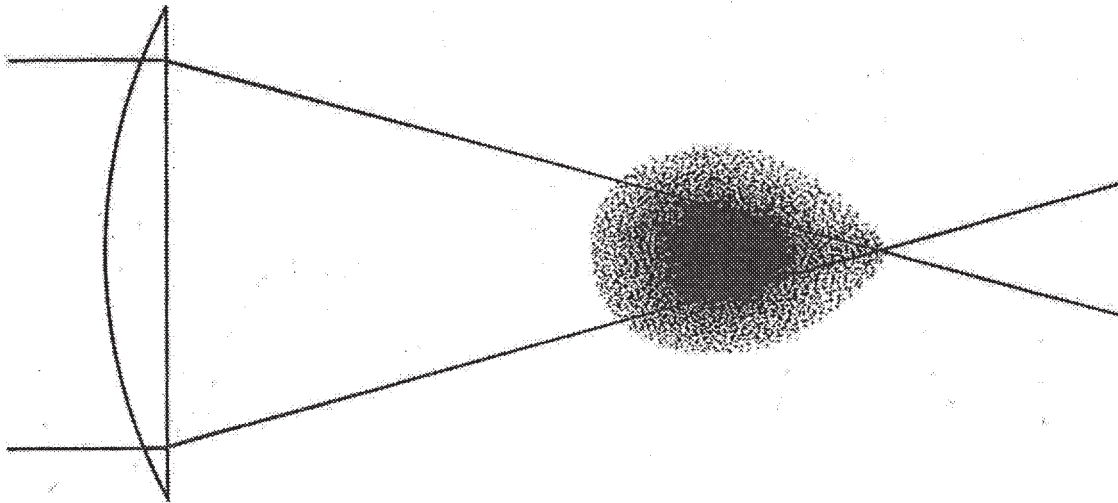
Continuous, laser-sustained plasmas have been produced in a variety of gases at pressures from 1 to 210 atm using carbon dioxide lasers operating at a wavelength of $10.6\ \mu\text{m}$ and powers from 25 W to several kilowatts. Most of these experiments were performed in open air or large chambers with little flow, except for that provided by natural convection, but recent experiments by Gerasimenko et al. (1983), Welle et al. (1987), and Cross and Cremers (1986) have demonstrated that the LSP can be operated successfully in a forced convective flow. Gas discharges that operate in a flowing environment have been called "plasmatoms" in the Soviet literature, and the laser-sustained plasma is often referred to as an "optical plasmatron." These experiments have demonstrated that plasma conditions are strongly dependent on the position of the plasma within the sustaining beam, and that the plasma can be controlled within a wide range of conditions using appropriate combinations of laser power, flow, and optical configuration.

The unique ability to sustain a plasma within a small, isolated volume at relatively high pressures and temperatures has suggested a number of potential applications for the laser-sustained plasma. Since the LSP can operate in pure hydrogen and the power can be beamed remotely, it has been proposed that the LSP could be used for high specific-impulse space propulsion. A number of papers have dealt with this application, and it was the subject of a review by Glumb and Krier (1984). Thompson et al. (1978) described experiments in which laser energy was converted into electrical energy using a laser-sustained argon plasma. Cremers et al. (1985) have suggested the LSP as a source for spectrochemical analysis and given some experimental results. Cross and Cremers (1986) have sustained plasmas in the throat of a small nozzle to produce atomic oxygen having a directed velocity of several km/sec for the laboratory study of surface interactions at energies and particle fluxes similar to those experienced by satellites in low-earth orbit. Other applications are suggested by analogy to other plasma devices including light sources, plasma chemistry, and materials processing.

The physical processes that determine the unique characteristics of the LSP will be discussed in Sec. 4.2, and the theoretical analyses that have been used to describe the LSP will be addressed in Sec. 4.3. Experimental results obtained will be presented in Sec. 4.4 and compared with the theoretical predictions. Sec. 4.5 will consider some possible applications.



(a)



(b)

Figure 4.1 (a) Photograph of a plasma sustained by a 600 W carbon dioxide laser beam focused with a 191 mm focal length lens. (b) Schematic representation showing how the plasma forms within the focal volume.

4.2 PRINCIPLES OF OPERATION

Plasmas that are created or sustained by lasers can be generated in a variety of forms, depending on the characteristics of the laser and optical geometry used to generate them. High-energy pulsed lasers can generate plasma breakdown directly within a gas that results in a transient expanding plasma similar to an explosion. At lower laser intensities and longer pulse times, plasmas may be initiated at solid surfaces and then propagate into the sustaining beam at supersonic velocities as a laser-sustained detonation (LSD) wave or subsonic velocities as a laser-sustained combustion (LSC) wave. These transient plasmas have been discussed by Raizer (1980) and will not be treated here. If the laser is continuous in output power and the optical geometry, flow, and pressure are favorable, then a steady-state LSP may be continuously maintained at a position near the focus of the beam. The intensity that is available from a continuous laser is insufficient to cause breakdown in the gas, however, and an auxiliary source must be used to initiate the plasma. A sketch of a steady-state laser-sustained plasma is shown in Fig. 4.1(b). The plasma may be sustained within a confining chamber to control the flow and pressure or in open air or a large chamber where the flow is determined by thermal buoyancy.

In many ways, the laser-sustained plasma is similar to direct current or low-frequency electrodeless arcs and microwave discharges that are operated in similar gases and at similar pressures. However, the LSP will generally be more compact and have a higher maximum temperature than other continuous arc sources and can be sustained in a steady state well away from containing boundaries. A fundamental difference in the way in which energy is absorbed by the plasma is responsible for these unique characteristics of the LSP.

4.2.1 Basic Physical Processes

In a direct current (dc) arc or in an inductively coupled plasma (ICP), energy is absorbed through ohmic heating produced by the low-frequency or direct currents flowing in the plasma. The electrical conductivity of an ideal plasma is given by (Shkarofsky et al., 1966)

$$\sigma = \frac{ne^2}{m} \left(\frac{\nu - i\omega}{\nu^2 + \omega^2} \right) \quad (4.1)$$

where n is the electron density, e the electronic charge, m the electron mass, ω the radian frequency of the applied electric field, ν the effective collision frequency for electrons, and i the square root of -1 . In the dc arc ($\omega = 0$), the currents are transmitted through the plasma between electrodes and

the size of the plasma is determined by the size and spacing of the electrode and the confining boundaries. In the ICP, the currents are induced into the plasma from alternating currents flowing in a surrounding solenoidal coil. The arc is sustained within a container that determines the plasma diameter, whereas the length of the plasma is determined by the length of the solenoid.

The ICP operates at frequencies well below the plasma frequency

$$\omega_p = \left(\frac{ne^2}{m\epsilon_0} \right)^{1/2} \quad (4.2)$$

where ϵ_0 is the permittivity of free space. In this frequency range, the electromagnetic field does not propagate as a wave within the plasma, but is attenuated as an evanescent wave (Holt and Haskell, 1965) over distances of the order of the skin depth

$$\delta = \frac{c}{\sqrt{\omega_p^2 - \omega^2}} \quad (4.3)$$

where c is the speed of light. Thus, the plasma is sustained by energy absorbed within a small layer near its outer surface that produces a rather flat temperature profile within the plasma and limits the maximum temperatures that can be obtained.

The frequency of the optical fields (28 THz for the 10.6 μm carbon dioxide laser) used for the LSP is greater than the plasma frequency, and therefore the incident laser beam can propagate well into the interior before it is significantly absorbed through the process of inverse bremsstrahlung (Shkarofsky et al., 1966). Since the focusing of the laser beam produced by a lens or mirror is essentially preserved as the beam propagates into the plasma, very large field strengths may be produced within the plasma near the beam focus. It is these large field strengths that lead to peak temperatures in the LSP that are generally greater than those obtained with either dc arcs or the ICP and make it possible to sustain a small volume of plasma near the focus, well away from any confining walls.

Inverse bremsstrahlung is a process in which the plasma electrons absorb photons from the laser beam during inelastic collisions with ions, neutrals, and other electrons. The collisions between electrons and ions are the dominant process for the LSP and the absorption coefficient is given by (Shkarofsky et al., 1966)

$$\alpha = \left(\frac{\pi c}{\omega} \right)^2 \frac{nS_0 G}{kT} \left(\frac{1 - e^{-\hbar\omega/kT}}{\hbar\omega/kT} \right) \quad (4.4)$$

where \hbar is Planck's constant divided by 2π , k Boltzmann's constant, and T the temperature of the electrons. The factor G is the Gaunt factor and the factor nS_0 is given by

$$nS_0 = \frac{16 n_+ n Z^2}{3 m^2 c^3} \left(\frac{e^2}{4\pi\epsilon_0} \right)^3 \left(\frac{2\pi m}{3kT} \right)^{1/2} \quad (4.5)$$

where Z is the ionic charge and n_+ the ion density. The Gaunt factor is a quantum mechanical correction to the classical theory, and extensive tables have been given by Karzas and Latter (1961). For the usual case where the photon energy is much less than the thermal energy ($\hbar\omega \ll kT$), the bracketed term in Eq. (4.4) is nearly independent of ω , and the absorption coefficient is essentially proportional to the square of the wavelength.

The size of the LSP will depend on several factors including the beam geometry, laser power, and absorption coefficient. The change in intensity of the laser beam as it propagates within the plasma is given by Beer's law

$$\frac{dI}{ds} = -\alpha I \quad (4.6)$$

where s is the distance along the local direction of propagation. The absorption length $1/\alpha$ is a dominant length scale for the LSP since it determines the distance over which the power is absorbed from the beam. For this reason, the dimension of the high-temperature absorbing portion of the plasma along the laser beam will be of the order of the absorption length. Although it is the absorption length that determines the length of the plasma along the beam axis, it is the laser beam diameter that determines the plasma diameter. The plasma expands to fill the beam cone where it is able to absorb power, then rapidly decreases in temperature outside the beam through thermal conduction and radiative loss mechanisms.

The position of the LSP relative to the focal point is critical in determining its structure and the range of parameters for which it can be maintained. When the plasma is initiated near the beam focus, it propagates into the sustaining beam and seeks a stable position. The position of stability will be located where the beam intensity is just sufficient that the absorbed power will balance the losses due to convection, thermal conduction, and thermal radiation. A number of factors combine to determine this position of stability including the transverse profile of the incident beam, the focal length and aberrations of the focusing lens or mirror, the plasma pressure, and the incident flow velocity (Keefer et al., 1986; Welle et al., 1987).

The power per unit volume that is absorbed by the plasma is given by

$$P = \alpha I \quad (4.7)$$

where I is the local irradiance of the laser beam. Since I depends on the transverse profile of the incident beam as well as the focal length and aberrations of the lens, these characteristics will influence the location within the focal region at which the minimum sustaining intensity is located. For example, for a small f /number lens, the intensity decreases rapidly with increasing distance from the focus and the plasma will stabilize near the focus. For a larger f /number system, the intensity decreases less rapidly and the plasma will stabilize at a position further away from the focus. Indeed, for sufficiently long focal lengths and high laser power, plasmas have been observed to propagate many meters (Razier, 1980) as "laser-supported combustion waves" at subsonic velocities.

The detailed spatial structure of the plasma is determined by the interrelations between the optical geometry of the sustaining beam, the pressure of the gas, and the flow through the plasma. At each point within the plasma, the temperature and flow must adjust to balance the power that is absorbed from the laser beam with the power lost through convection, conduction, and thermal radiation. The position in the beam relative to the focal point at which the plasma stabilizes is very important in determining the structure of the plasma that, in turn, determines the conditions of power, pressure, and flow for which a stable plasma can be maintained.

Most of the early experiments with the LSP were carried out inside large chambers or in open air, where the flow through the plasma was determined by the effects of thermal buoyancy. Fixed focal geometries were used and the pressure and laser power were varied to define regions of power and pressure where it was possible to sustain the LSP in a variety of gases (Generalov et al., 1972; Kozlov et al., 1979; Moody, 1975). These experiments indicated that there were upper and lower limits for both laser power and pressure at which the LSP could be sustained.

Generalov et al. (1972) suggested that the upper limit for power was a result of forming the LSP with a horizontal beam. In this geometry, thermal buoyancy induces a flow transverse to the optical axis. The induced flow carries the plasma up and out of the beam when higher laser power causes the plasma to stabilize farther from the focus. They were unable to establish an upper power limit when the experiment was operated with the beam propagating vertically upward. Kozlov et al. (1974) developed a radiative model for the LSP and explained the upper power limit on the basis that the plasma must stabilize close enough to the focal point that the geometric increase of laser beam intensity going into the plasma was greater than the loss of intensity due to absorption. They speculated that the failure of Generalov et al. (1972) to observe this limit in a vertical beam was due to rapid extinction and reignition of the plasma.

It is clear from the experiments of Generalov et al. (1972) that flow can have a large effect on the range of pressure and laser power that will support

a stable LSP. Plasmas sustained in the free jet issuing from a nozzle have been studied by Gerasimenko et al. (1983) who measured the discharge wave velocity along the beam and ranges for the existence of a steady-state discharge. Recently, experiments have been conducted in confined tubes where forced convection dominated the flow (Welle et al., 1987). It was found that in addition to power and pressure, both the flow and optical geometry of the beam have a profound influence on the characteristics of the plasma. It now appears that the earlier experimental results that defined regions of pressure and power for which the LSP could be sustained are valid only for the particular experimental geometry used to obtain them.

When the plasma is ignited by an auxiliary source near the focal point, the plasma expands as it absorbs energy from the continuous laser beam and propagates into the beam with decreasing velocity until it stabilizes. The plasma becomes stationary at a point where the intensity is just sufficient that the power absorbed from the beam, given by Eq. (4.7), is balanced by the convective, conductive, and radiation losses. Since, in general, the intensity is not uniform across the beam, the plasma will adjust in size, shape, temperature, and flow to satisfy conservation of momentum and energy. If the flow through the plasma increases, then the thermal convection losses increase in the upstream region of the plasma and it must move toward the focus to a region of higher intensity in order to absorb enough power from the beam to compensate for the increased convective losses.

Thermal radiation plays a significant role in determining the detailed structure of the plasma. Thermal radiation in the plasma occurs both as a result of bound-bound transitions, resulting in line radiation and absorption, and free-bound and free-free transitions that result in continuum radiation and absorption. Over the optically thin portion of the spectrum, this radiation will not be strongly absorbed by the plasma or surrounding cooler regions and will simply escape from the plasma. Other portions of the spectrum will be strongly absorbed, resulting in a transport of energy within the plasma. In the optically thick limit, this results in a diffusive energy transport that is similar to thermal conduction, but may be significantly larger. Detailed calculations of the LSP (Jeng and Keefer, 1986) indicate that this radiative transport is a dominant factor in the determination of the structure and position of the LSP. In particular, it is the radiative transport that determines the temperature gradient in the upstream front of the plasma, thereby determining the position in the beam for which convection losses are balanced by absorption.

The position of stability for the LSP also depends on the plasma pressure. The absorption coefficient is a strong function of plasma density, as seen from Eq. (4.4). If the pressure is increased and the absorption coefficient increases, then the plasma can absorb more power from the beam and will move away from the focus to a lower intensity region in the beam. At the

same time, the plasma length along the beam decreases because of the decrease in absorption length, but the diameter increases to fill the larger cross section of the beam. Thus, for the same laser beam conditions, a higher-pressure LSP will stabilize at a point farther away from the focal point and have a smaller length-to-diameter ratio than a lower-pressure LSP.

Incident laser power, as well as the *f*/number and aberrations of the focusing optics, will also influence the position at which the LSP stabilizes within the beam. From the foregoing discussion, it is clear that as the beam power is increased, the plasma will move up the beam away from the focal point. The distance that it moves is determined by the *f*/number (ratio of focal length to the beam diameter incident on the focusing element) of the optical system, since the rate of change in beam intensity along the optical axis decreases with an increase in *f*/number. Lens aberrations can also have an effect on plasma position (Keefer et al., 1986). In particular, when an annular beam from an unstable laser oscillator is focused by a spherical lens, it produces an annular prefocus region before reaching the focal point, and the intensity in this region may be sufficient to sustain an annular plasma.

From the observations discussed above, it is clear that the position of the plasma relative to the focal point has a profound effect on the plasma characteristics. At the upper limits of stability for both laser power and pressure, it appears that the plasma becomes unstable when it moves too far from the focal point. This may be due to the fact, as proposed by Kozlov et al. (1974), that as the plasma moves sufficiently far away from the focus, the rate of increase of the beam intensity in the direction of propagation becomes smaller. Since the temperature of the plasma must increase as the beam propagates into the upstream edge of the plasma, the intensity of the beam must also increase. At some point, the decrease of the beam intensity due to absorption is greater than the increase due to focusing, so the plasma becomes unstable and extinguishes. Recent calculations by Jeng and Keefer (1987a), however, indicate that there may exist local regions within the LSP where the beam intensity decreases as it penetrates the plasma.

A considerable degree of control of the structure and position of the LSP can be gained through both optical geometry and flow, in addition to laser power and pressure. Utilization of these additional parameters makes it possible to successfully operate the LSP over a wider range of experimental conditions, enabling a wider range of potential applications.

4.2.2 Plasma Characteristics

Laser-sustained plasmas have been operated in a variety of molecular and rare gases at pressures from 1 to more than 200 atm. The resulting plasmas have characteristics that are similar to arc plasmas operated at similar pres-

tures, but the peak temperatures in the LSP are usually somewhat higher than those for the comparable arc. Radiation from the plasma can be a significant fraction of the total power input, and radiation transport plays a major role in determining the structure of the plasma. Continuum absorption processes are of particular importance in these plasmas since the power to sustain the plasma is absorbed through these mechanisms.

The continuum absorption process involves both bound-free transitions (photoionization) and free-free transitions (inverse bremsstrahlung) in which photons are absorbed from the laser beam. The free-free transitions involve electron collisions with ions, other electrons, and neutral particles (Shkarofsky et al., 1966; Griem, 1964). The dominant absorption process for the LSP is through collisions between electrons and ions, and the absorption coefficient for this process is given by Eq. (4.4). For the usual case in the LSP, $\hbar\omega \ll kT$ and the absorption is approximately proportional to the square of the laser wavelength. Due to this strong wavelength dependence, all of the reported experimental results for the LSP have been obtained using the 10.6 μm wavelength carbon dioxide laser. Since the length scale for the plasma is of the order of the absorption length, the length of the plasma and the power required to sustain it would be expected to increase dramatically for shorter wavelength lasers. Currently, the only other lasers that are likely candidates to sustain continuous plasmas are the hydrogen or deuterium fluoride chemical lasers that operate at wavelengths of 3 to 4 μm .

Thermal radiation is one of the most important characteristics of the LSP. Thermal radiation lost from the plasma can account for nearly all the power absorbed by the plasma when the flow through the plasma is small and will account for a significant fraction of absorbed power even when the convective losses are large. The thermal radiation consists of continuum radiation resulting from recombination (free-bound transitions) and bremsstrahlung (free-free transitions) as well as line radiation (bound-bound transitions). Calculation of this radiation is straightforward, although rather tedious, when the plasma is in local thermodynamic equilibrium (LTE) (Griem, 1964). Local thermodynamic equilibrium is established when the electron collisional rate processes dominate the processes of radiative decay and recombination. When LTE is established in the plasma, the density in specific quantum states is the same as a system in complete thermal equilibrium having the same total density, temperature, and chemical composition. It should be emphasized that this does not imply that the radiation is similar to a blackbody at the plasma temperature. In general, the spectrum of the radiation from the plasma will have a complex structure consisting of the superposition of relatively narrow spectral lines and a continuum having a complex spectral structure.

The absorption coefficient in the plasma depends on the wavelength, and for the ultraviolet portion of the spectrum below the wavelength of the resonance lines (transitions involving the ground state), the radiation is strongly absorbed by the plasma and the cooler surrounding gas. This results in a strong radiative transport mechanism that is important in determining the structure of the plasma. Often, radiative transport for strongly absorbing gases is modeled as a diffusive energy transport similar to thermal conduction. In the strongly ionized regions of the plasma, the radiative transport is many times larger than the intrinsic thermal conduction and is the dominant heat-transfer mechanism. This is especially true in the upstream region of the LSP where the temperature gradient is large, and radiation transport must offset the convective losses of the incident flow.

In the longer wavelength region above the resonance transitions, the absorption of the radiation by the plasma and the surrounding gas is much smaller. The absorption length for this radiation is often large compared to the characteristic dimensions of the plasma, and much of the radiation escapes. In this region of the spectrum, the plasma may be considered optically thin, and if the plasma is in LTE, then the escaping radiation can be used to characterize the temperature within the LSP (Keefer et al., 1986; Welle et al., 1987).

The temperature within the plasma is far from uniform, as shown in Fig. 4.2. (The method used to obtain the experimental temperatures shown in Figs. 4.2, 4.4, and 4.10 is described in detail in Sec. 4.4.2). This figure shows an isotherm plot of the temperatures measured in an LSP sustained in 2.5 atm of argon by a carbon dioxide laser operating at a wavelength of $10.6 \mu\text{m}$. The plasma length and diameter, as determined by the 10,500K isotherm, are 11 and 4 mm, respectively. Note the steep temperature gradients that exist in the upstream portion of the plasma and in the radial direction near the limit of the laser beam. The temperature gradients in these regions are of the order of 10^6 K/m . In the upstream regions of the plasma, the direction of the convective energy transport is the opposite of that due to thermal conduction and radiation transport, and a strong temperature gradient develops to balance the convective losses with thermal conduction and radiative transport. The magnitude of the temperature gradient depends on the flow rate and increases with increasing flow. Strong radial temperature gradients develop near the edge of the laser beam where the available power decreases rapidly and are steeper near the focus where large conduction and radiation transport is required to balance the large powers absorbed from the beam. The peak temperature in the plasma occurs near focus where the laser beam intensity is maximum, and the peak temperature has a value that corresponds closely to the temperature at which the first stage of ionization is nearly complete. The correspondence of the maximum temperature with complete first ionization is to be expected since, for a constant pres-

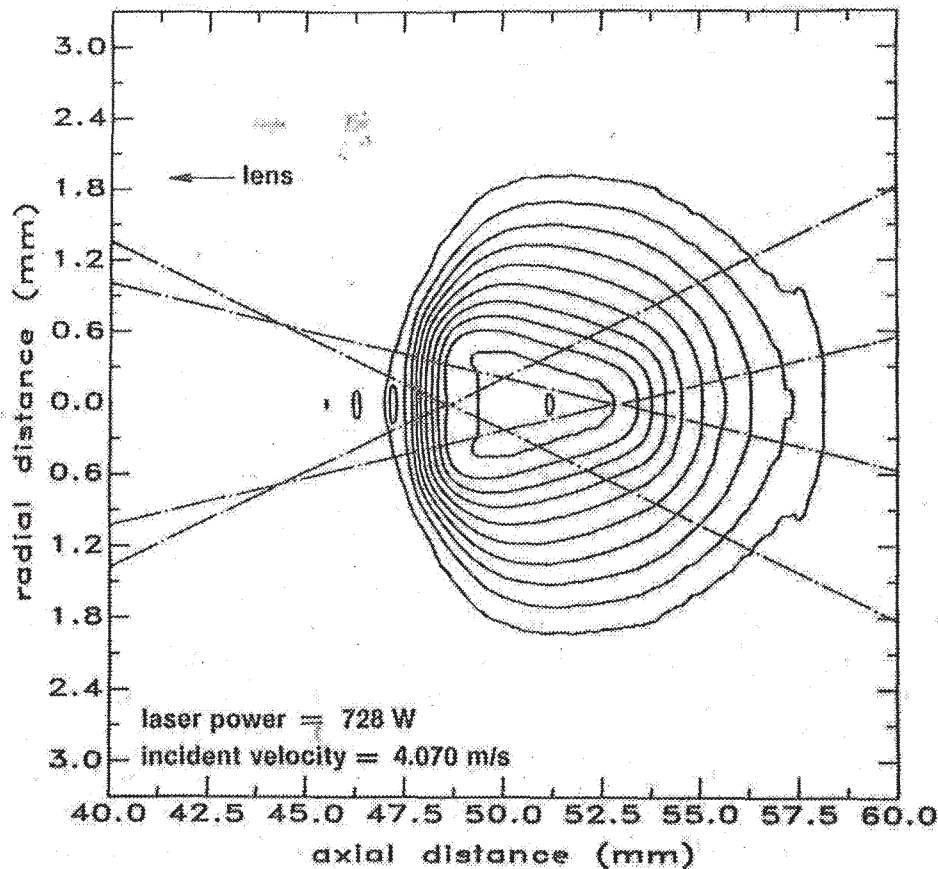


Figure 4.2 Measured isotherms for a 2.5 atm argon plasma sustained by an annular beam from a carbon dioxide laser focused by a lens of 203 mm focal length. The horizontal scale was arbitrarily chosen so the focus occurs at 50 mm, and both the laser beam and the flow are incident from the left. The contour interval is 500K with the outer contour at 10,500K. (From Welle, R., et al., 1987, Copyright © American Institute of Aeronautics and Astronautics; reprinted with permission.)

sure plasma, the absorption coefficient passes through a maximum at that temperature.

Plasmas have been sustained by carbon dioxide lasers in a variety of gases including the rare gases xenon, argon, and neon and in several molecular gases including hydrogen, deuterium, nitrogen, carbon dioxide, and air. Plasmas in the heavier rare gases (xenon, krypton, and argon) are the easiest to sustain since they have relatively low ionization potential, their thermal conduction is relatively small, and no dissociation energy must be supplied. Few experiments have been reported using the lighter rare gases, but Carloff et al. (1981) have sustained optical discharges in helium and neon to pressures of 207 atm and Cross (1986) has operated a discharge in

neon with admixtures of oxygen. Relatively higher laser powers were required with helium to offset the greater ionization potential and relatively large thermal conductivity. The molecular gases also require greater laser power since these gases must absorb sufficient energy to undergo dissociation before they can be ionized. As discussed earlier, the threshold power required to maintain a plasma depends on the details of the experiment including beam quality, optical geometry and aberrations, and the flow rate. For example, Generalov et al. (1972) found the threshold power for argon at a pressure of 10 atm to be approximately 90 W, whereas Moody (1975) found the threshold to be approximately 30 W at the same conditions. For a single experimental configuration, Kozlov et al. (1979) found the threshold increased going from argon to nitrogen to air to deuterium to hydrogen.

4.2.3 Practical Implementation

Application of laser-sustained plasmas has not been widespread, and most of the operational systems have been constructed in research laboratories to study the plasma itself. The LSP has been used in an experimental attempt to measure the high-temperature absorption of mixtures of water vapor and hydrogen (Fowler, 1981). Cross (1986) has used the LSP to generate very high-speed molecular oxygen beams for the study of satellite surface interactions, and Cremers et al. (1985) have used the LSP as a source for atomic spectroscopy. Recently, detailed laboratory studies of the LSP have been conducted by Keefer et al. (1986), Welle et al. (1987), and Krier et al. (1986) to determine their suitability for laser thermal propulsion.

The experiments with continuous laser-sustained plasmas have been performed using focused beams from continuous carbon dioxide lasers with output powers between a few tens of watts and several tens of kilowatts. The simplest way to create the LSP is to focus the beam from the laser into ambient air using a lens or mirror. If the power is approximately 5 kW or greater, a plasma can be initiated by a discharge near the focal point that is created by an arc, a pulsed laser plasma breakdown, or by momentarily placing a metallic (usually tungsten) surface in the focal volume. The stability of the LSP is enhanced by operating the beam so that it is propagating vertically upward toward the focus. This insures that the flow induced by thermal buoyancy is in the same direction as the beam propagation and does not tend to convect the hot plasma out of the high-intensity focal region. Various focal length lenses have been used to focus the beam, with typical systems having focal lengths from 25 to 300 mm and f /numbers from 1.5 to 5. Plasmas have been sustained using beams of various mode structures: annular beams produced by unstable oscillators, multimode beams from stable oscillators, and Gaussian beams. There has been little system-

atic study of the influence of beam quality on the LSP, but in general the threshold power required to sustain the plasma decreases with increasing beam quality. Moody (1975) has sustained plasmas in argon at pressures greater than 10 atm using only 25 W from a laser having a Gaussian beam that was focused by a mirror of 52 mm focal length. Various investigators have reported threshold values that vary by a factor of 10 or more, and many of these differences are probably due to the variety of beam quality and focusing geometries that have been employed.

To operate the LSP in gases other than air and at pressures greater than 1 atm, it is necessary to confine the plasma within a chamber. Often, these have been chambers that were large compared to the plasma, and the flow in the plasma has been established by the thermally induced, free convective flow within the chamber. Recent experiments have been conducted (Krier et al., 1986; Welle et al., 1987) in which argon plasmas were sustained in a forced convective flow. The forced convective flow velocity was considerably larger than the thermally induced flow velocities, and it was found that the plasmas could be sustained over a wide range of power and pressure by adjusting the flow velocity and optical geometry.

4.3 ANALYTICAL MODELS

Soon after laser-induced breakdown was discovered, theoretical models for breakdown of a gas in an optical field were developed by Zel'dovich and Raizer (1965). Raizer (1965) then developed a model for the supersonic propagation of the absorption wave, and later (Raizer, 1970) developed a one-dimensional model for the subsonic propagation and maintenance of a laser-sustained plasma. This model was based on an analogy with combustion, and these subsonic propagating waves, together with the continuous laser-sustained plasmas, became known in the United States as "laser-supported combustion waves (LSC)." The closed-form solution for this model was widely used to interpret experimental observations of propagating plasmas, but was found to greatly underestimate the observed propagation velocity.

The Raizer model was extended by Jackson and Nielsen (1974) to include the effect of radiative transfer, and they obtained a numerical solution that led to much better agreement between the predicted propagation velocities and experimental observations. Kozlov and Selezneva (1978) developed a one-dimensional, time-dependent model and studied numerically the transition of the plasma from the initiation spark to a stationary discharge. Kemp and Root (1979) extended the Jackson and Nielsen (1974) model to predict the characteristics of a hydrogen LSP for laser propulsion. The numerical methods that were used by Jackson and Nielsen

(1974) and Kemp and Root (1979) led to a divergence of the solution near the maximum temperature, and Keefer et al. (1985) applied a new method of numerical solution that provided converged solutions throughout the solution domain. It was clear from all of the numerical models that radiative transfer in the forward portion of the propagating plasma played a dominant role in the determination of the propagation velocity.

Batteh and Keefer (1974) developed a quasi-two-dimensional model for the LSP that was based on an extension of the Raizer analysis. They included the effect of radial and axial thermal conduction and finite laser beam diameter, but assumed that the laser beam was collimated and radial components of the flow could be neglected. The closed-form solutions for the temperature that were obtained agreed qualitatively with observed plasmas. This model was extended by Muller and Uhlenbusch (1982) to include the important effect of the convergence of the laser beam geometry. They used a focused Gaussian beam to model the two-dimensional, axisymmetric distribution of laser intensity in the focal region. Approximate solutions were obtained for the case in which the influence of the containing walls was neglected and restricted functional forms of the transport properties were used.

A more elaborate model of the flow in the vicinity of the LSP was developed by Carloff et al. (1984). They obtained solutions of the Navier-Stokes equations for the thermally induced buoyant flow within a closed chamber containing the plasma. The solution was obtained for the flow within the cooler gas region outside of the high-temperature plasma core by solving the momentum equations using a temperature field that was calculated separately. The temperature field was obtained from a solution of the energy equation using an assumed Gaussian beam profile and a velocity field obtained from the momentum equations using an assumed temperature profile. The equations were not coupled, and it was not clear whether the radiation and transport properties had an assumed spatial variation or whether the temperature- and pressure-dependent properties were used. Their solutions clearly showed the recirculation cells that develop in the closed chamber and the deflection of the streamlines around the high-temperature plasma core.

The next step in the development of two-dimensional models was taken by Glumb and Krier (1985) who included the effect of focusing by assuming a uniform convergent beam focused to an arbitrary spot size and retained the assumption that radial components of the flow could be neglected. However, they obtained numerical solutions using fully coupled temperature- and pressure-dependent transport properties. This model produced predicted temperature fields that were similar to those observed and gave good results for global absorption of laser power.

Merkle (1984) developed a theoretical model to consider the case in which the plasma was sustained in a chamber having a converging-diverging nozzle. He solved the quasi-one-dimensional Navier–Stokes equations numerically using an implicit time-marching method for a plasma mixture of hydrogen, cesium, and water. Beam convergence was included in an approximate fashion but radiation transfer was neglected. A model that contained a complete two-dimensional description of the flowfield was developed by Molvik et al. (1985), but the flowfield was uncoupled from the radiation by the assumption of a constant absorption coefficient. This assumption was relaxed by Merkle et al. (1985) by assuming absorption into a mixture of hydrogen, cesium, and water that exhibits strong absorption at relatively low temperatures. They were unable to obtain convergence for pure gases because of the strong gradients and nonlinear temperature-dependent properties.

Jeng and Keefer (1986) developed a full two-dimensional model based on a Navier–Stokes description of the flowfield, geometric ray-tracing for laser beams of arbitrary radial profiles, and a radiative transfer model that divided the radiative transport into optically thick and optically thin regions. This model was solved numerically using the SIMPLE (Jeng and Keefer, 1986) algorithm for pure argon in a pipe flow where the plasma was sustained by the annular beam from an unstable resonator. These solutions were found to be in good agreement with detailed measurements, and the model was extended to obtain solutions for plasmas sustained in hydrogen by Gaussian laser beams (Jeng et al., 1987). Comparison of the solutions obtained using the full two-dimensional model with those obtained from the quasi-two-dimensional model, in which the radial components of the flow are neglected, clearly show that the full two-dimensional treatment of the flowfield is required for accurate predictions. Due to the pressure increase caused by the strong heat addition, the flow is diverted around the outside of the plasma core and the mass flow through the plasma core may be reduced by a factor of 5 or more compared with the simpler models (Jeng et al., 1987). This effect is shown in Fig. 4.3 where the temperature isotherms are shown in the upper half of the figure, and the local mass flux is represented by the vectors in the lower half. This calculation was for a 3 atm hydrogen plasma sustained by a 20 kW, 40 mm diameter Gaussian beam from a carbon dioxide laser operating at 10.6 μm .

Development of the detailed two-dimensional models has made it possible to gain considerable insight into the factors that control the LSP. One factor that was found to be of considerable importance is the characteristics of the laser beam and the focusing optics. It was found, both experimentally and from the model, that when an annular beam from an unstable oscillator was used to sustain the plasma, spherical aberrations caused an annular prefocus ahead of the focal point, and that this high-intensity region could

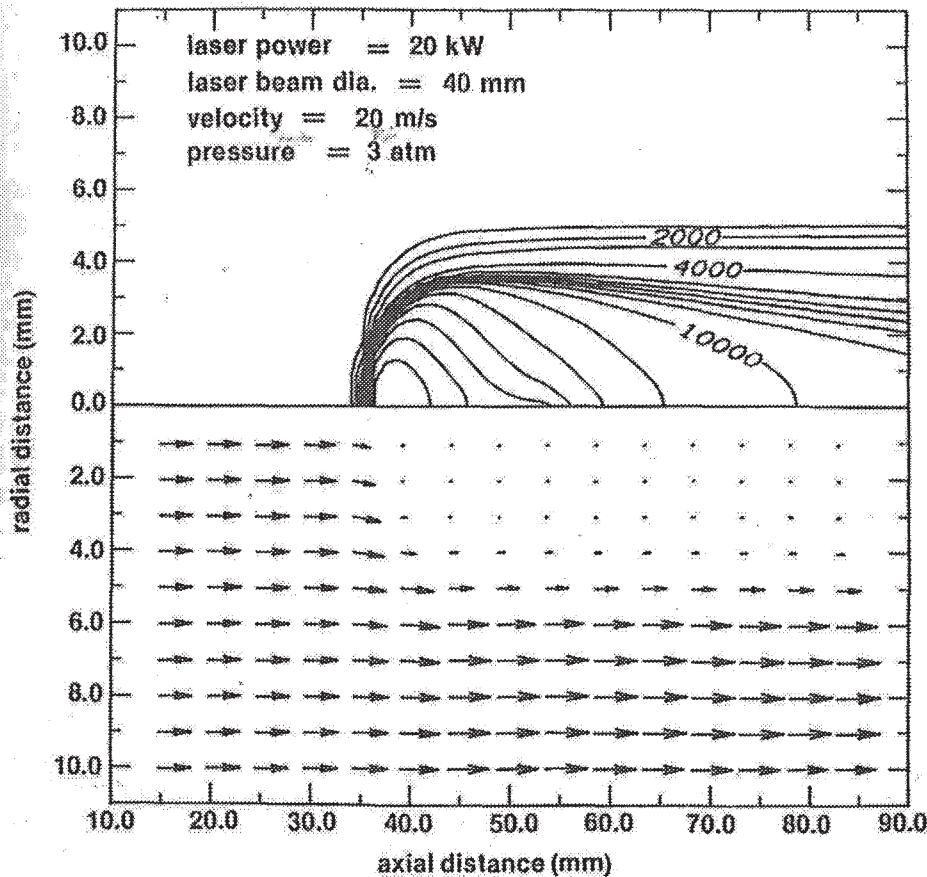


Figure 4.3 Theoretical calculation for a hydrogen plasma sustained by a 40 mm diameter Gaussian beam focused by a 203 mm focal length lens to the 50 mm position on the horizontal axis. The incident flow velocity is 20 m/sec in a cylindrical pipe 22 mm in diameter. The upper part of the figure contains isotherms and the lower half contains vectors whose length and direction represent the local mass flux (product of local density and local velocity). (From Jeng, S. M. and Keefer, D., 1987a. Copyright © American Institute of Aeronautics and Astronautics; reprinted with permission.).

sustain a plasma that had significant off-axis temperature maxima. An example of this effect is shown in Fig. 4.4. The upper half of the figure shows the measured isotherms and the lower half shows the isotherms predicted by the model. It is seen from the figure that the plasma is sustained further from the focus than that shown in Fig. 4.2, and that off-axis temperature maxima occur near the annular prefocus indicated by the crossing of the limiting rays of the annular beam, indicated by the dashed lines.

The models have also shown that the f /number of the focusing lens has an important effect on the fraction of laser power that is absorbed by the

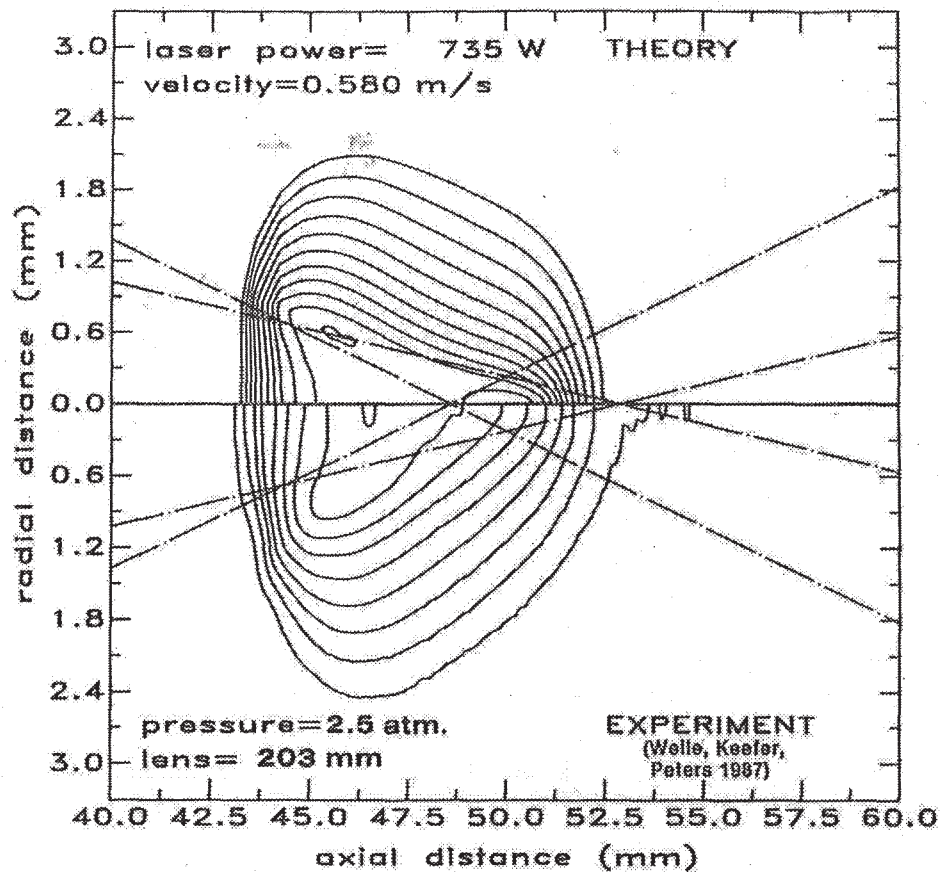


Figure 4.4 Comparison between measured and calculated isotherms for an argon plasma sustained with an annular beam. Both the laser beam and the flow are incident from the left. Off-axis maxima in the temperature appear where the spherical aberration of the lens causes a high-intensity annular prefocus. (From Jeng, S. M., et al., 1987. Copyright © American Institute of Aeronautics and Astronautics; reprinted with permission.)

plasma and the fraction of absorbed power that is lost from the optically thin plasma through radiation. As the f -number of the optical system is increased, the diameter of the plasma will be smaller if there is sufficient incident flow velocity to sustain the plasma near the focal region. This smaller volume plasma will lose less power by thermal radiation and can absorb more power from the beam because it is located in a region of higher laser intensity. The models predict that in hydrogen plasmas, it should be possible to sustain a plasma that absorbs virtually 100% of the incident laser beam power and that radiates no more than 35% of that power out of the plasma (Jeng et al., 1987).

Since all of the reported experimental data is for carbon dioxide lasers operating at a wavelength of $10.6\ \mu\text{m}$, the detailed models provide an opportunity to investigate the effects of using different wavelengths to sustain the plasma. An example is shown in Fig. 4.5 (Jeng, 1986). The upper isotherms are for a plasma sustained using a $10.6\ \mu\text{m}$ wavelength and the lower isotherms are for a plasma sustained with a wavelength of $3.9\ \mu\text{m}$ that is typical of chemical lasers. The incident power of $5245\ \text{W}$ for the $3.9\ \mu\text{m}$ wavelength has been scaled up from the incident power of $710\ \text{W}$ used to sustain the plasma at $10.6\ \mu\text{m}$ by the square of the ratio of wavelengths, to compensate for a similar decrease in the absorption coefficient. Note that for the shorter wavelength, the maximum temperature is considerably higher, and the plasma shape and size have changed. As discussed in Sec. 4.2.1, the plasma diameter is about the same for the two wavelengths,

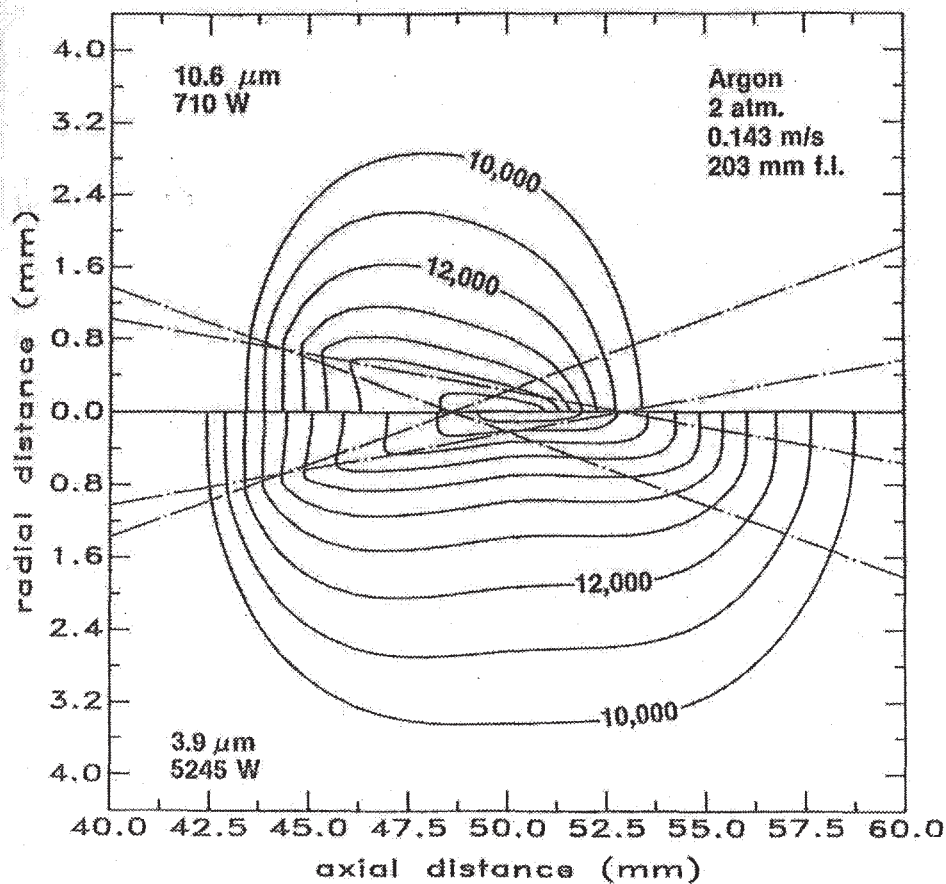


Figure 4.5 A comparison of calculated argon plasmas sustained by lasers of $10.6\ \mu\text{m}$ wavelength and $3.9\ \mu\text{m}$ wavelength. The incident power for the $3.9\ \mu\text{m}$ case was scaled upwards by the square of the ratio of the wavelengths to compensate for a similar reduction in the absorption coefficient.

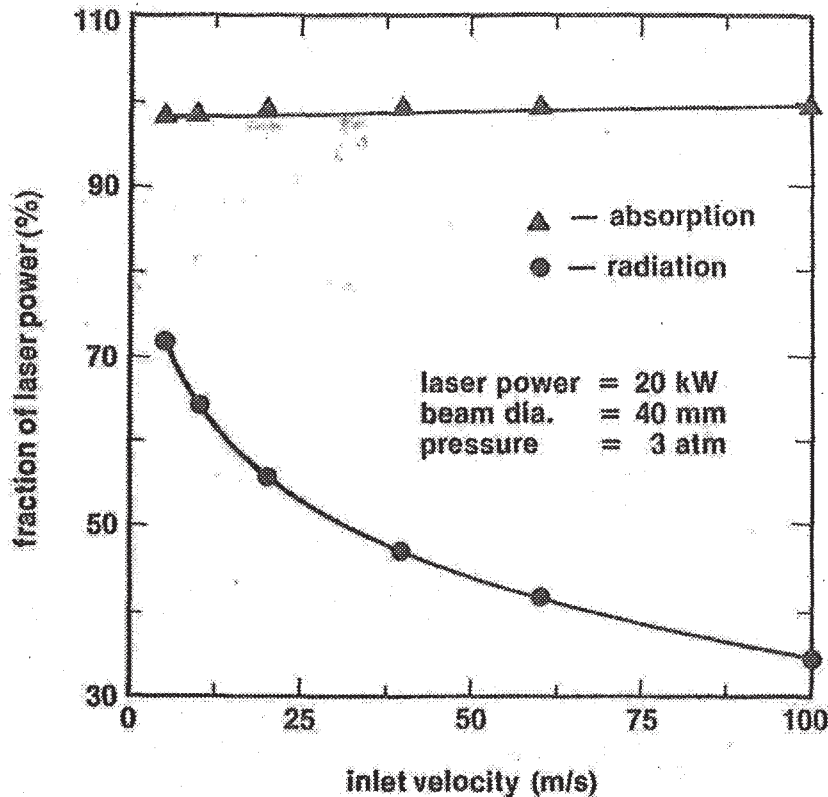


Figure 4.6 Calculated fractions of incident laser power that are absorbed and reradiated from a hydrogen plasma at a pressure of 3 atm. The plasma was sustained by a 20 kW Gaussian beam having a wavelength of $10.6 \mu\text{m}$. (From Jeng, S. M. and Keefer, D., 1987a. Copyright © American Institute of Aeronautics and Astronautics; reprinted with permission.)

since this is primarily a function of the beam diameter, but the length of the plasma has increased for the plasma sustained with the $3.9 \mu\text{m}$ beam due to the larger absorption length. A significant amount of laser power is absorbed beyond the focal point in this plasma that leads to a “dogbone” shape for the isotherms. The predicted fraction of incident power absorbed at $3.9 \mu\text{m}$ was 28%; considerably less than the prediction of 75% for $10.6 \mu\text{m}$.

The models also indicate that the plasma can be sustained over a wide range of flow velocities and that it is difficult to “blow out.” The flow velocity has a profound influence on the shape of the plasma and the position of the plasma within the beam. At low incident flow velocities, the plasma propagates up the beam becoming larger in diameter and volume and, therefore, more power is radiated out of the plasma region. When the incident flow velocity is increased, the plasma moves toward the focus, becoming smaller in diameter and somewhat longer in length. The result of

this change in plasma shape is a reduction in the power lost through radiation and an increase in power absorbed from the laser beam. This effect is shown in Fig. 4.6 where the calculated fraction of the power absorbed from the incident laser beam and the fraction of the incident power that is lost by radiation are shown as a function of the incident flow velocity. It is found that the fractional power absorption increases with incident flow velocity and, for these conditions, nearly all the incident power is absorbed. The absorption increases with velocity because the plasma is longer in the higher-velocity cases, and this increases the absorption pathlength. The fractional power that is lost from the plasma decreases as the incident flow velocity is increased. The power radiated from the plasma is proportional to the plasma volume and, since the diameter of the plasma is smaller for higher incident flow velocity, the radiating volume of the plasma is reduced.

The development of detailed numerical models has made it possible to study and interpret the complex interactions among optical geometry, flow, and pressure that occur within the LSP. The results of these studies indicate that the characteristics of the LSP can be controlled by a judicious choice of these parameters to produce plasmas in a wide variety of gases with plasma properties that can be optimized for a particular application. This detailed understanding, together with the increasing availability of industrial carbon dioxide lasers of good beam quality, should greatly expand the practical applications of the laser-sustained plasma.

4.4 EXPERIMENTAL STUDIES

Experimental studies of the LSP have been limited due to the requirement for continuous laser power above 1 kW and the lack of clearly identified applications. Until recently, most of the experimental studies were directed toward defining combinations of laser power, plasma material, and pressure for which the LSP could be successfully operated. Within the past few years, more detailed studies have been made that better elucidate the interactions among optical geometry, pressure, and flow that control the characteristics of the LSP.

4.4.1 Operational Parameters and Plasma Properties

The first systematic study of the LSP was reported by Generalov et al. (1972). They ignited the plasma using a pulse breakdown in argon or xenon produced by a pulsed and Q-switched carbon dioxide laser and then sustained the plasma with a continuous carbon dioxide laser having an unspecified beam and focusing configuration. The transition from the pulsed laser

spark to a continuous plasma was investigated and they measured propagation velocities of 10 m/sec that rapidly decreased to zero. It was found that the pulsed laser could also extinguish the LSP once it had been established, if the LSP was operating near threshold. They photographed the plasma and noted the change in shape and position of the plasma as a function of pressure and laser power. Stark broadening of the hydrogen H_β line was used, together with the Saha equation, to obtain estimates of the plasma temperature that ranged from 13,000 to 23,000K in argon plasmas.

The principal quantitative results of the Generalov et al. (1972) study was a determination of the regions of laser power and pressure for which continuous plasmas could be sustained in argon and xenon. Their measurements included pressures from 1 to 45 atm and laser power to 300 W. The threshold power was found to decrease rapidly with increased pressure in the range from 1 to 10 atm but was nearly constant at higher pressures. They attributed this pressure dependence of the threshold power to a transition of the dominant power loss mechanism from thermal conduction to thermal radiation. When the LSP was operated in a horizontal beam, they observed an upper pressure limit for existence of the LSP, but when operated in a vertical beam, no upper limit for pressure was observed. They attributed this result to the stabilizing effect of the thermally induced buoyant flow. Curiously, they also observed an upper limit for laser power at the higher pressures when the beam was operated horizontally, but they did not observe an upper power threshold when the beam was operated in a vertical orientation. These results for the horizontal beam are shown in Fig. 4.7. The curves for argon and xenon are similar in shape, but the argon curve is shifted to higher threshold power and pressure. Note that for xenon above 10 atm and argon above 18 atm, there was an upper limit of laser power for which the LSP was observed. The average laser power transmission was also measured, and it was estimated to be approximately 40% in these experiments. Carloff et al. (1981) extended the pressure range of these investigations to 210 atm for argon and helium, using a laser having good mode structure and focused with mirrors of short (1.5–2.5 cm) focal length.

Franzen (1972) and Moody (1975) conducted similar experiments with argon plasmas. Moody (1975) made a detailed study of the maintenance thresholds using a laser with good beam quality, and he further investigated the extinction of a continuous plasma when it absorbed a high-power laser pulse. Moody was able to sustain continuous plasmas in argon at pressures above 10 atm using a focal spot size of 80 μm diameter and incident powers as low as 25 W. Similar studies were extended to the molecular gases hydrogen, deuterium, nitrogen, and air by Kozlov et al. (1979), and the results were similar to those obtained for the rare gases except that the threshold power increased for the molecular gases.

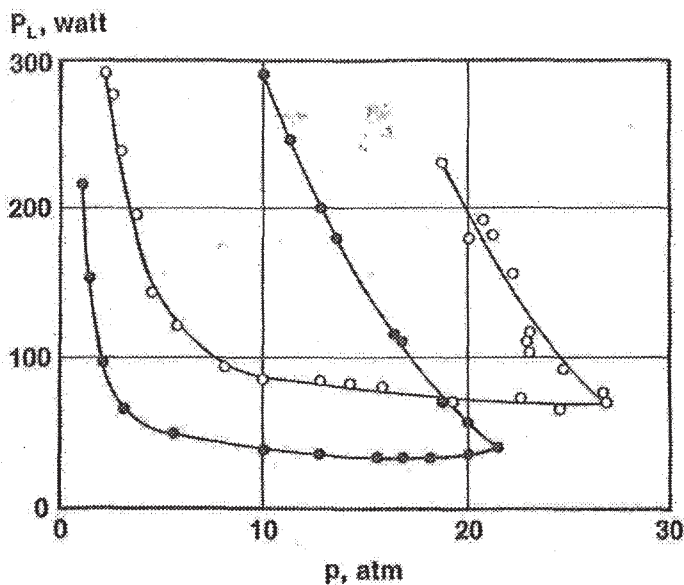


Figure 4.7 Experimentally measured minimum power required to sustain plasmas in argon (open circles) and xenon (closed circles). For argon above 18 atm and xenon above 10 atm there is also a maximum power for which the plasma can be sustained. (From Generalov, N. A., et al., 1972. American Institute of Physics; reprinted with permission.)

Klosterman and Byron (1974) performed experiments on plasmas in air that were initiated from metallic targets using relatively long pulses from a gasdynamic laser at powers to 400 kW. These plasmas were not stationary, but propagated into the beam at subsonic velocities. They measured the propagation velocity as a function of beam diameter and power, and these results were widely used to compare the early theoretical models for the laser-supported combustion wave (LSC). The observed velocities ranged from 10 to 50 m/sec and were much higher than those predicted by the one-dimensional model of Raizer (1970) when the radiation transfer was neglected. Similar measurements were also made by Fowler and Smith (1975) using well-characterized beams from continuous carbon dioxide lasers at powers to 15 kW, and they also studied the ignition thresholds for aluminum and steel targets in the presence of a transverse wind velocity to 20 m/sec.

Detailed measurements of the structure of the LSP were obtained by Fowler and Smith (1975) using interferometric methods, and by Keefer et al. (1975) using spectroscopic methods. The measurements were obtained for plasmas sustained in ambient air by a vertical beam from a continuous carbon dioxide laser operating at a nominal power of 6 kW. These results indicated that the maximum temperature in the plasma was approximately 17,000K with the 15,000K isotherm nearly coinciding with the outer

edge of the laser beam. The diameter of the 10,000K isotherm was approximately 10 mm, its length was approximately 14 mm, and the position of the temperature maximum was approximately 11 mm from the focus. Keefer et al. (1975) also found spectroscopic evidence that the plasma was not in LTE in the outer regions of the plasma where the temperature gradients were large.

4.4.2 Effects of Flow and Optics

Recent interest in the use of the LSP as a means to heat hydrogen for use in a high specific-impulse laser-powered rocket (Jones and Keefer, 1982; Caveny, 1984) has led to new and more detailed experimental studies. A primary objective of these studies has been to determine the absorption characteristics and stability of the plasma under the influence of forced convective flow.

Conrad et al. (1979) studied LSC waves in hydrogen that were initiated from a spark discharge. They also described experiments in ambient air in which a plasma was stabilized at different positions in a large f /number beam by flowing air under pressure in a direction opposite to the plasma propagation. They found that the laser power transmitted by the plasma varied from nearly 100%, near the threshold irradiance of 9 kW/cm^2 , to nearly zero, when the average laser irradiance exceeded 20 kW/cm^2 . These results, not widely available, were crucial for the propulsion application of the LSP, since they indicated that virtually 100% of the laser power could be absorbed by the plasma if the flow configuration was correct.

Measurements of the flow velocity in the cooler regions surrounding the high-temperature plasma core were obtained by Carloff et al. (1984) using a laser Doppler anemometer. The plasma was sustained in argon within a closed cell, and it was observed that a thermal buoyancy driven recirculation cell developed in the chamber. The measured velocity field near the plasma showed that the streamlines were deflected outward around the high-temperature core of the plasma. They found that the velocity far from the plasma core was about 5 cm/sec and increased near the plasma to 20 cm/sec. A more detailed investigation of the effect of flow on the range of power and pressure for which the LSP could be maintained was reported by Gerasimenko et al. (1983) who also established that the discharge wave velocity exhibited a minimum value.

Experiments were conducted with flowing argon by Krier et al. (1986) using a 10 kW materials processing laser. The annular beam from the unstable oscillator was focused into a 137 mm diameter chamber by a complicated system of mirrors that permitted variation of the f /number of the focused beam between 2.2 and 3.4. Mass flow rates of 2.3 to 4.6 g/sec pro-

vided bulk flow velocities from 11 to 22 cm/sec. Detailed temperature measurements of the outer regions of the flow below 3000K were made using tungsten-rhenium thermocouples. Measured isotherms were presented for two pressures, 1.1 atm and 3.3 atm, and two incident laser powers, 3.3 and 6.5 kW. They also measured the plasma absorption using a water-cooled copper cone calorimeter and found that the fractional absorption of the laser beam approached 80% at the higher laser powers.

Detailed spectroscopic measurements of the plasma region above 10,000K were obtained by Keefer et al. (1986) for plasmas sustained in a vertical flow of argon by a 1.5 kW CO₂ laser. The plasmas were sustained in a quartz tube of 22 mm diameter having a conical entrance section. The experimental apparatus is shown in Fig. 4.8. Digital images of the plasma continuum emission in a 1 nm bandpass centered at 626.5 nm, a spectral region free of line emission, were acquired at video frame rates (60/sec) using a digital image processing computer. These images were Abel-inverted to obtain plasma emission coefficients that could be related to the plasma temperature using an assumption of LTE. Geometric ray tracing through the measured temperature field provided a spatially resolved measurement of the power absorption from the laser beam. They found little effect of flow within the range of 0.8 to 32 cm/sec incident flow velocity, which is in the range of the velocities induced by thermal buoyancy. For this limited range of incident flow velocity, they found that the flow had little influence on the characteristics of the plasma. The detailed spatial measurements, for plasmas sustained with an annular beam focused by lenses of 203 and 305 mm focal length, revealed the importance of spherical aberrations on the structure of the plasma. They also found that the pressure dependence of the plasma was considerably different for the two lenses and concluded that experimentally determined threshold values were specific to the optical geometry used. Fig. 4.9 shows the pressure dependence of fractional power absorption observed using focusing lenses of two different focal lengths. Note that, for the longer focal length lens, the absorbed power decreases sharply near a pressure of 2 atm. Indeed, it was not possible to sustain a plasma above 2 atm using the 305 mm focal length lens and a volume flow of 3.2 standard L/min.

This experimental investigation was extended by Welle et al. (1987) to include incident convective velocities up to 4.5 m/sec, considerably larger than those induced by thermal buoyancy. At the higher flow velocities, the plasma shape, size, and position within the focal volume were significantly influenced by the forced convection. Fig. 4.10 shows that, in the case of low flow, the plasma stabilized at a position well away from the focal point and developed off-axis temperature maxima. The off-axis maxima were created by the relatively high intensity in an annular ring that resulted from spherical aberrations. With an increase in the incident flow velocity, the plasma

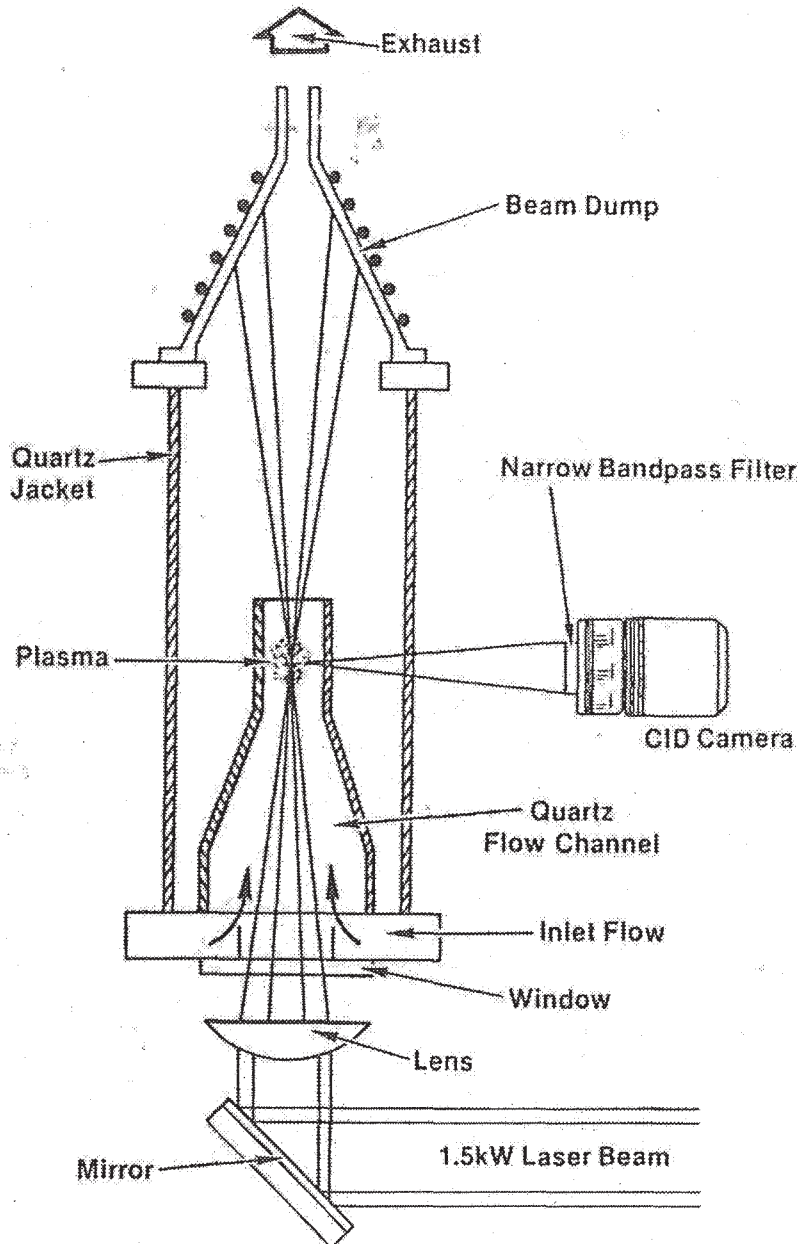


Figure 4.8 Experimental apparatus used to obtain detailed spectroscopic temperature measurements in a flowing argon LSP. (From Keefer, D., et al., 1986. Copyright © American Institute of Aeronautics and Astronautics; reprinted with permission.)

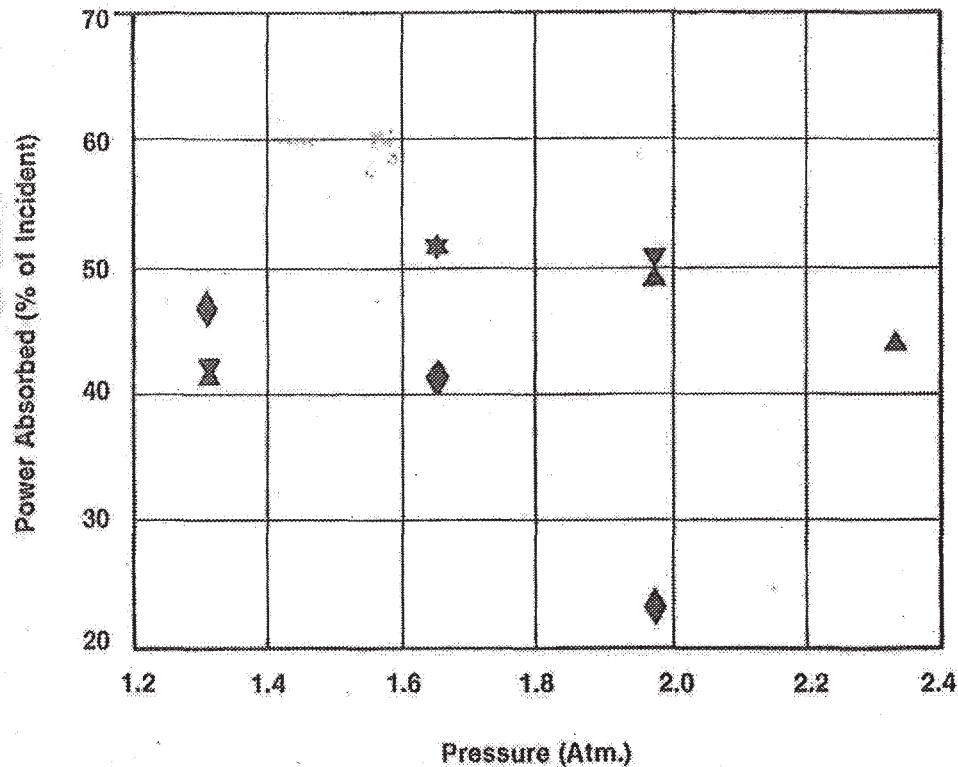


Figure 4.9 Fractional power absorption as a function of pressure for three sets of plasmas: 203 mm focal length, 3.2 std. liters/min (\blacktriangle); 203 mm focal length, 9.6 std. liters/min (\blacktriangledown); 305 mm focal length, 3.2 std. liters/min (\blacklozenge). The incident power was 710 W. (From Keefer, D., et al., 1986. Copyright © American Institute of Aeronautics and Astronautics; reprinted with permission.)

stabilized at a position much nearer the focal point, away from the annular prefocus. The region of maximum temperature was more compact and was positioned within the region of maximum beam intensity. Because of the smaller volume of the high-temperature region, the radiation loss decreased from 53 to 45% of the incident radiation, and since the higher-temperature portion of the plasma stabilized in a higher-intensity portion of the beam, the power absorption increased from 67 to 78% of the incident beam power. This effect has significant implications regarding the regions of power and pressure for which the LSP can exist. For example, although it was impossible to sustain a plasma above 2 atm using the 305 mm focal length lens and 3.2 standard L/min flow, the plasma could be sustained with this lens at pressures above 2 atm when the incident flow velocity was increased.

Detailed analyses of a large number of laser-sustained plasmas have revealed the complex interactions between the flow and the energy conversion processes within the plasmas. These experiments suggest that stable laser-

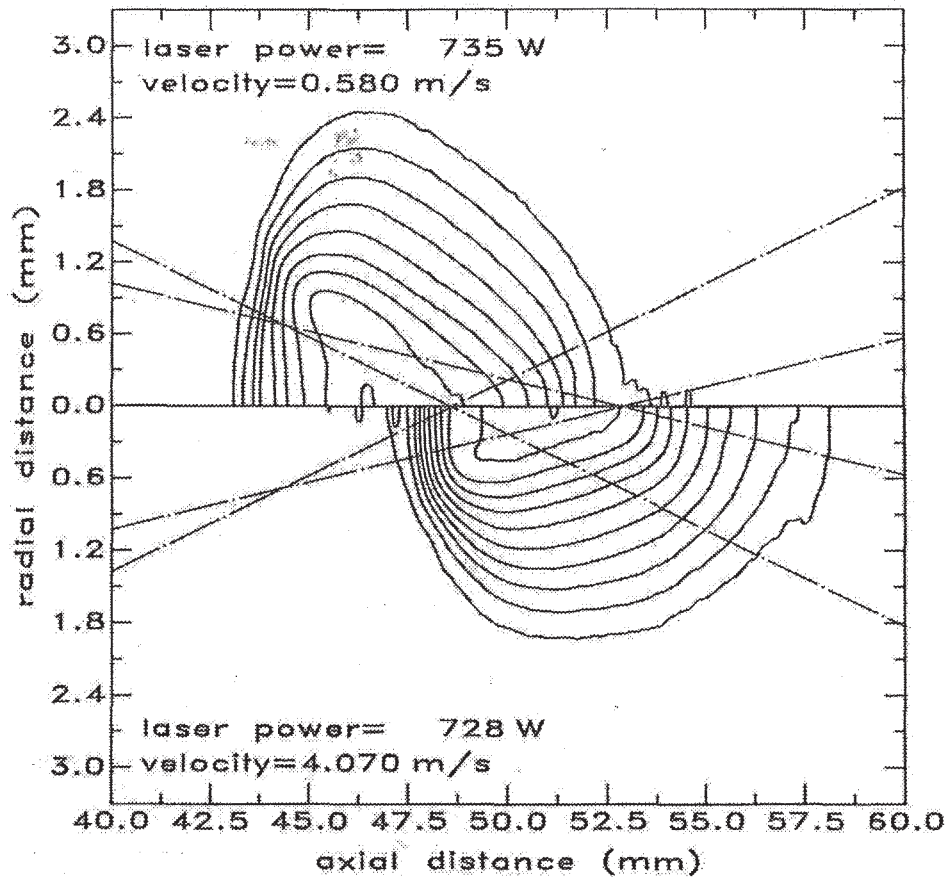


Figure 4.10 The effect of incident flow velocity on the measured isothermal contours for two plasmas sustained using a 203 mm focal length lens in argon at a pressure of 2.5 atm. The upper plasma was sustained in an incident flow velocity of 0.58 m/sec while the lower plasma was sustained in an incident flow velocity of 4.07 m/sec. The contour interval is 500K, with the outer contour at 10,500K. (From Welle, R., et al., 1987. Copyright © American Institute of Aeronautics and Astronautics; reprinted with permission.)

sustained plasmas may be operated over a wider range of conditions than previously reported by using appropriate combinations of optical geometry, pressure, and incident flow velocity.

4.5 APPLICATIONS OF THE LASER-SUSTAINED PLASMA

Although the laser-sustained plasma can produce small, well-controlled, continuous plasmas in a variety of gases having peak temperatures greater than those produced by the ICP or dc arcs, there have been few reported

applications. This is probably due, in part, to the fact that the high-power carbon dioxide lasers used to sustain the plasmas are relatively expensive and have not been widely available. In recent years, this situation has been changing as the carbon dioxide laser has found increasing acceptance by industry for various materials processing applications, and it is likely that new applications will increase in the future.

4.5.1 Laser Propulsion

The concept for using the power beamed from a laser for rocket propulsion was proposed by Kantrowitz (1971) and Minovitch (1972). Some early research on this concept was carried out, primarily by AVCO Everett Laboratories and Physical Sciences, Inc. These applications, however, required very large laser power (1 to 1000 MW) and interest waned until recently, when research on the free-electron laser suggested that these large laser powers were possible. A review of the early work on the laser propulsion concept was given by Glumb and Krier (1984) and, in a special volume edited by Caveny (1984), several chapters were devoted to the use of beamed laser power to provide propulsion for orbit raising missions. New experimental investigations of laser-sustained plasmas were begun at NASA Marshall Spaceflight Center, The University of Tennessee Space Institute, and the University of Illinois. A theoretical study was undertaken at the University of Pennsylvania. The objectives of the experimental studies were to develop an understanding of the basic physical processes involved in the stability and power absorption of the LSP in a flowing gas. The goal of the theoretical work was to develop numerical methods that could deal with the strong gradients of density and temperature and the strong coupling of the plasma transport and thermal properties that exist in the LSP. Many of the results from these recent investigations have been discussed in the preceding sections.

The use of a LSP to absorb the power from a laser beam and to convert it to enthalpy in the propellant gas has been called laser thermal propulsion (Keefer et al., 1984). This refers to the concept in which power from a laser is beamed to a vehicle where it is absorbed by the LSP and used to heat a pure hydrogen propellant to provide thrust at large values of specific impulse (1000 to 1500 sec). With these high specific-impulse values, the fractional payload that can be delivered from low-earth orbit (LEO) to geosynchronous earth orbit (GEO) is significantly larger than that achieved by chemical propulsion systems. Furthermore, the mass of the propulsion system can be smaller than other high specific-impulse systems (e.g., nuclear or electric propulsion) since the source of power is beamed to the vehicle from a remote site.

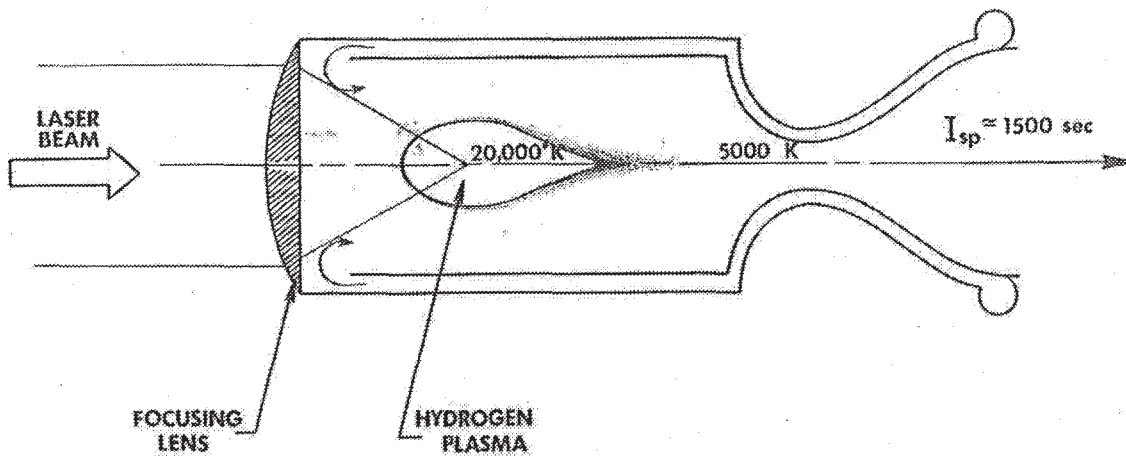


Figure 4.11 Schematic representation of a rocket motor that operates by laser thermal propulsion. It is predicted that the specific impulse (I_{sp}) from such a motor may be several times greater than that obtained from conventional rocket motors.

A schematic representation of the rocket motor is shown in Fig. 4.11. The incoming laser beam is focused into the absorption chamber where it sustains a plasma at temperatures of approximately 16,000 to 20,000K. In contrast to a normal combustion chamber, the high-temperature plasma occupies only a small fraction of the chamber volume and mixes with the incoming propellant to produce a flow having a bulk temperature of approximately 3000 to 5000K that can be expanded through the nozzle to produce thrust. Due to the high temperature of the LSP, a substantial portion of the absorbed power will be radiated from the plasma and absorbed by the chamber walls. In order to utilize this radiated power effectively, the chamber walls are cooled by the incoming propellant in a regenerative cycle. If the power radiated from the plasma can be limited to that required to raise the propellant from storage temperature to an acceptable inlet temperature, then all of the absorbed power can be utilized to heat the propellant and no external radiator will be required. Sufficient mixing of the inlet propellant and the high-temperature region within the LSP must be insured to produce the bulk temperature required for the nozzle inlet and to minimize the radial temperature gradients in the nozzle flow.

The fraction of absorbed laser power that is lost from the plasma as thermal radiation has a profound influence on the performance that can be achieved by the thruster (Keefer et al., 1987). If the acceptable inlet temperature limits the enthalpy of the inlet flow to h_0 , then the final bulk enthalpy will be limited to $h_T = h_0/\alpha_{RAD}$, where α_{RAD} is the fraction of the absorbed laser power that is radiated to the walls by thermal radiation. The final bulk enthalpy and, therefore, the specific impulse of the thruster

will be determined by the radiated fraction of the absorbed laser power that may be absorbed by regenerative cooling. It is clear that the success of this concept rests on the ability to sustain a stable plasma in a forced convective flow that can absorb substantially all of the incoming radiation and to limit the fraction of the absorbed laser power that is lost from the plasma region through thermal radiation.

Another factor that will affect the performance of this rocket concept is the radial temperature distribution at the nozzle throat. Due to the strong radial temperature gradients associated with the LSP, unless there is sufficient mixing downstream of the plasma with the surrounding colder buffer flow, there will be a much higher-temperature core near the axis in the throat. This results in an inefficient utilization of the absorbed power to produce thrust, with a corresponding loss in specific impulse. Jeng and Keefer (1987b) have developed a new computational model that spans the subsonic to supersonic flow regime to study these effects.

Recent, detailed experiments with the LSP in a forced convective flow have revealed the complex interactions between the flow, pressure, and laser power that determine the stable operating regimes for these plasmas. It was found that the position of the plasma within the focal volume of the laser beam could be controlled with the incident flow velocity. Controlling the flow, together with the focusing geometry of the laser beam, permits stable operation of the plasma with high fractional absorption of the incident laser beam and relatively small thermal radiation losses from the plasma.

Numerical models that incorporate the complex energy conversion processes within the plasma have been developed and verified using the detailed experimental measurements. Results from these model calculations indicate that hydrogen plasmas can be sustained that will absorb essentially all of the incident laser power and will lose a sufficiently small fraction of the absorbed power through thermal radiation. The numerical studies for hydrogen plasmas indicate that when higher-power Gaussian laser beams are employed, the chamber walls can be adequately cooled by the propellant flow in an efficient regenerative cycle. No "fatal flaws" have been discovered by either the experimental or theoretical investigations, and it appears that a practical, high specific-impulse propulsion system could be based on the laser thermal propulsion concept, if lasers having adequate power are developed and suitable window materials can be found.

4.5.2 Atomic and Molecular Beams

A device, similar in configuration to a laser thermal rocket motor, has been used by Cross and Cremers (1985 and 1986) to produce high-particle flux beams of xenon, argon, and atomic oxygen. The objective of this research

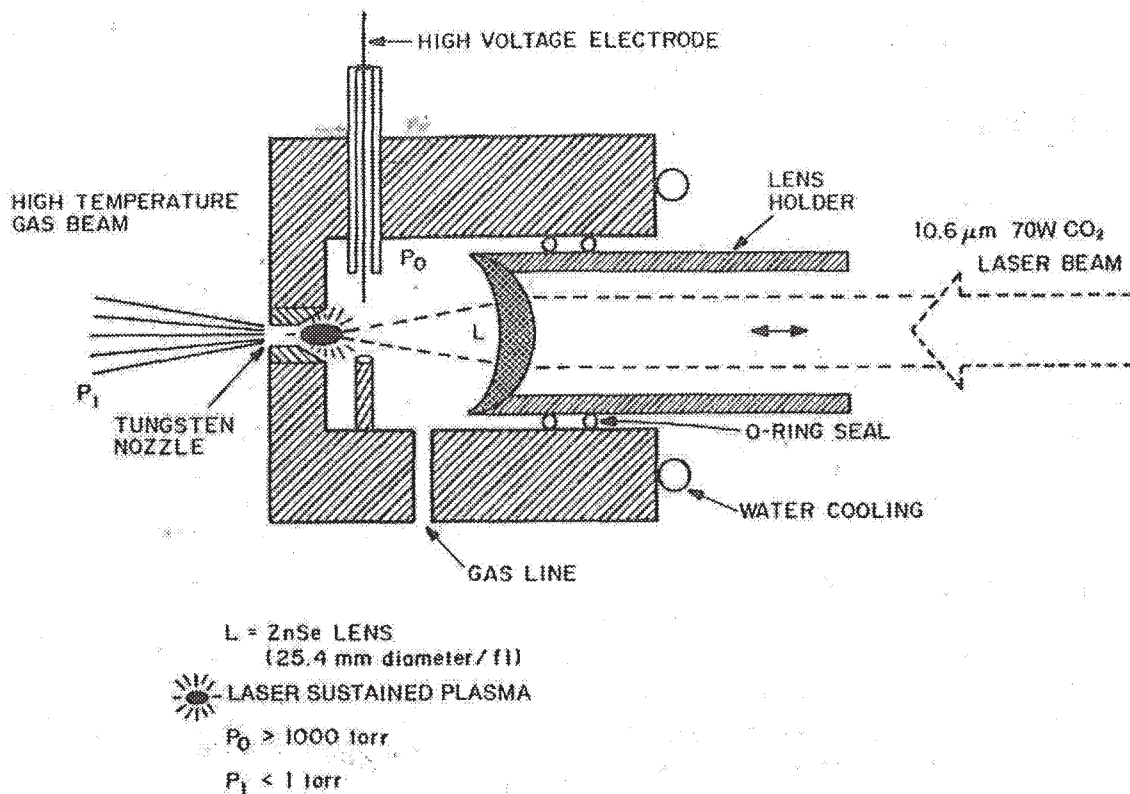


Figure 4.12 Schematic of a high velocity molecular beam source that utilizes a laser-sustained plasma. (From Cross, J. B. and Cremers, D. A., 1985. Copyright © American Institute of Aeronautics and Astronautics; reprinted with permission.)

is the production of atomic oxygen beams that can be used to study the interaction of oxygen atoms with spacecraft surfaces at velocities and particle fluxes similar to those encountered in the orbital environment.

The plasma is sustained in a chamber near a small diameter nozzle as shown in Fig. 4.12. The gasdynamic expansion of the high-temperature gas into a vacuum produces a high-velocity molecular beam. Time of flight measurements using xenon and a laser power of 70 W showed that the beam temperature (velocity) increased dramatically as the plasma is moved closer to the nozzle as shown in Fig. 4.13. The resulting xenon beam had a velocity of 1.34 km/sec and an absolute intensity estimated at 10^{19-20} particles/sec-sr. A platinum nozzle was developed for use with higher laser powers and mixtures containing oxygen. This beam was operated at powers to 500 W, but the time of flight measurements was not reported. Based on their results with xenon, the authors estimate that velocities of 3.6 km/sec can be

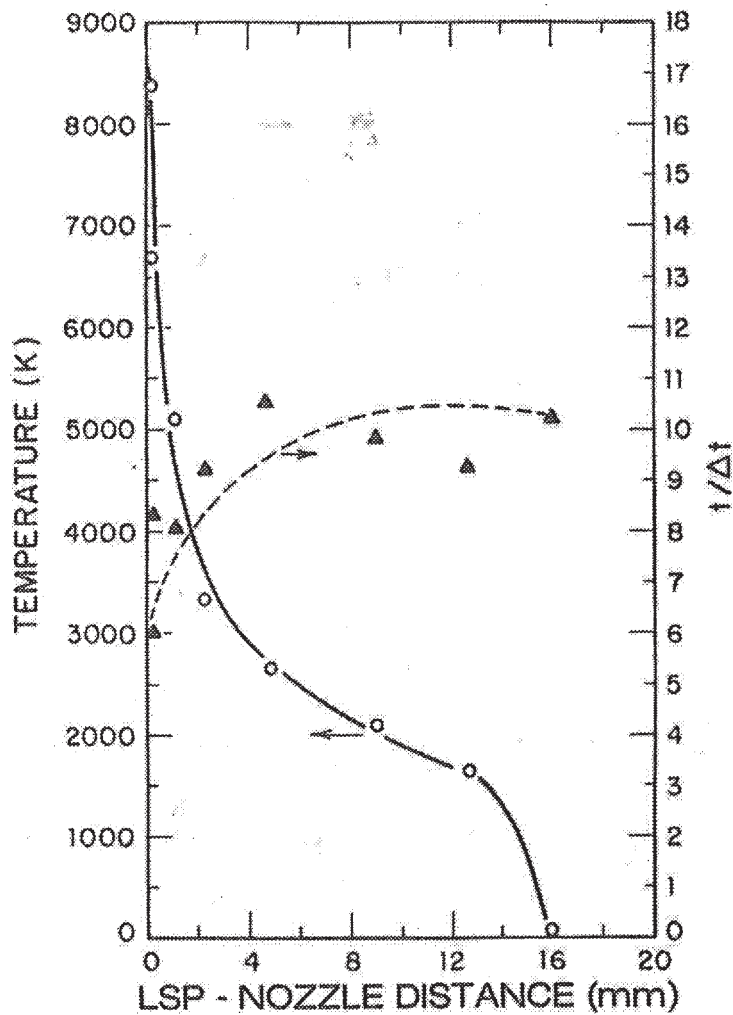


Figure 4.13 Variation of beam temperature and $(t/\Delta t)$ as a function of the plasma to nozzle distance for a xenon beam sustained with a 70 W laser. The data were obtained from an analysis of time-of-flight data. (From Cross, J. B. and Cremers, D. A., 1986. North-Holland Physics Publishing, Amsterdam; reprinted with permission.)

obtained using argon, 6 km/sec using neon, and 14.8 km/sec using helium as the carrier gas.

4.5.3 Spectrochemical Analysis

Various kinds of gas discharge plasmas, including dc arcs, ac arcs and sparks, the ICP, and microwave discharges, have long been used as excitation sources for atomic emission spectroscopy. As described in the pre-

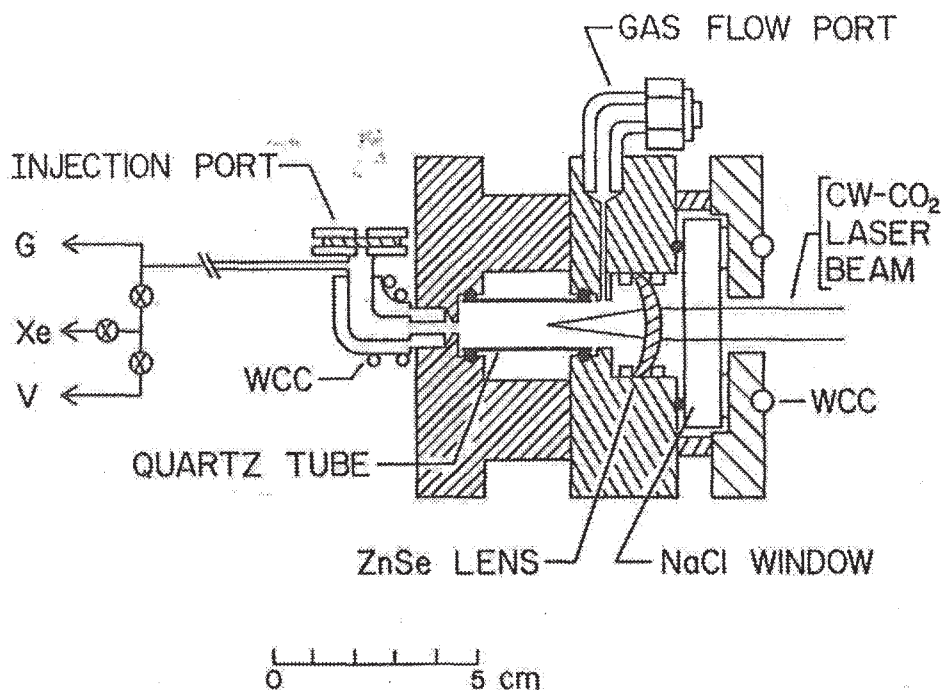


Figure 4.14 Diagram of the small gas cell that was used in analytical experiments with a static xenon fill. Gas samples were introduced through the injection port using a syringe. Solid samples were laser ablated from a metal strip located below the LSP. Here WCC is a water cooling coil, G is a pressure gauge, and V is a vacuum pump. (From Cremers, D. A., et al., 1985. Pergamon Press, Ltd.; reprinted with permission.)

ceding sections, the LSP produces a continuous high-temperature plasma that is free of electrode contamination, and it is natural to assume that it could also be used as an excitation source. The use of the LSP as a source for emission spectrochemical analysis has been evaluated by Cremers et al. (1985) who generated the plasma in xenon using a 45 W carbon dioxide laser.

They used two similar cells, the smaller of which is shown in Fig. 4.14. A monochromator, together with a chopper and lock in amplifier, was used to record the spectrum from the plasma. The plasma was initiated using the laser spark generated by focusing the pulse from a 2 MW, Nd:YAG laser. It was found that stable xenon plasmas could be maintained from 1150 to 3200 Torr using a laser beam power of 45 W. Detailed spectra of xenon from 200 to 950 nm were obtained for various conditions of power and pressure. The electron density was measured by seeding the discharge with a small amount of hydrogen and using the broadening of the H_{α} line. The plasma temperature was determined from a Boltzmann plot using the

emission lines from xenon and krypton that were added to the discharge gas. Their results were consistent with an assumption of LTE within the plasma. The stability of the emission was determined, and for the small cell the background (continuum) emission was found to have a relative standard deviation (RSD) of 0.3 to 0.6%, and for the 788.74 nm Xe I line the RSD was 0.42%.

Chlorine and oxygen were added to the xenon discharge and calibration curves were obtained for O and Cl atoms. It was found that as much as 10% by volume of chlorine or oxygen could be added to the xenon without noticeably affecting the discharge. Several solid compounds were introduced into the discharge by pulsed laser ablation from a steel substrate located below the LSP. Approximate detection limits were determined and found to be higher than those reported for the ICP. The authors conclude that there are several advantages of the LSP for spectrochemical analysis, but a more detailed performance evaluation should be carried out using argon as the carrier gas and operating the LSP as a plasmatron.

4.5.4 Other Potential Applications

The LSP is capable of generating a stable, contamination-free plasma at temperatures and pressures comparable to, or exceeding, that of dc arcs in a variety of gases over a wide range of pressures and flow. In addition, it is possible to generate small plasmas with absorbed powers that range from a few watts to tens or hundreds of kilowatts. Electric discharge plasmas have found numerous applications in chemical synthesis and materials processing and, with the increasing commercial availability of suitable lasers, it is reasonable to expect that similar applications will be found for laser-sustained plasmas.

REFERENCES

- Batteh, J. H. and Keefer, D. R. (1974). Two dimensional generalization of Raizer's analysis for the subsonic propagation of laser sparks, *IEEE Trans. Plasma Sci.*, PS-2: 122.
- Carloff, C., Krametz, E., Schafer, J. H., Uhlenbusch, J., and Wroblewski, D. (1981). Continuous optical discharges at very high pressure, *Physica*, 103c: 439.
- Carloff, C., Gillet, C., Krametz, E., Muller, A., Schafer, J. H., and Uhlenbusch, J. (1984). Theoretical description and measurement of the flow field of a continuous optical discharge, *Arch. Mech.*, 36: 473.
- Caveny, L. H., Ed. (1984). *Orbit Raising and Maneuvering Propulsion: Research Status and Needs*, ALAA Progress in Astronautics and Aeronautics series, Vol. 89, Washington, D.C.

- Conrad, R. W., Roy, E. L., Pyles, C. E., and Mangum, D. W. (1979). Laser-supported combustion wave ignition in hydrogen, Tech. Rep. RH-80-1, U.S. Army Missile Command, Redstone Arsenal, Alabama.
- Cremers, D. A., Archuleta, F. L., and Martinez, R. J. (1985). Evaluation of the continuous optical discharge for spectrochemical analysis, *Spectrochimica Acta*, 40B: 665.
- Cross, J. B. (1986). Private communication.
- Cross, J. B. and Cremers, D. A. (1985). Ground-based investigations of atomic oxygen interactions with space station surfaces, AIAA Paper 85-1068, AIAA 20th Thermophysics Conf., Williamsburg, Va.
- Cross, J. B. and Cremers, D. A. (1986). High kinetic energy (1–10 eV) laser sustained neutral atom beam source, *Nucl. Instrum. Meth. Phys. Res.*, B13: 658.
- Fowler, M. C. (1981). Measured molecular absorptivities for a laser thruster.
- Fowler, M. C. and Smith, D. C. (1975). Ignition and maintenance of subsonic plasma waves in atmospheric pressure air by CW CO₂ laser radiation and their effect on laser beam propagation, *J. Appl. Phys.*, 46: 138.
- Franzen, D. L. (1972). CW gas breakdown in argon using 10.6- μ m laser radiation, *Appl. Phys. Lett.*, 21: 62.
- Generalov, N. A., Zimakov, V. P., Kozlov, G. I., Masyukov, V. A., and Raizer, Y. P. (1970). Continuous optical discharge, *Sov. Phys. JETP Lett.*, 11: 302.
- Generalov, N. A., Zimakov, V. P., Kozlov, G. I., Masyukov, V. A., and Raizer, Y. P. (1972). Experimental investigation of a continuous optical discharge, *Sov. Phys. JETP*, 34: 763.
- Gerasimenko, M. V., Kozlov, G. I., and Kuznetsov, V. A. (1983). Laser plasmatron, *Sov. J. Quant. Electron.*, 13: 438.
- Glumb, R. J. and Krier, H. (1984). Concepts and status of laser-supported rocket propulsion, *J. Spacecraft and Rockets*, 21: 70.
- Glumb, R. J. and Krier, H. (1985). A two-dimensional model of laser-sustained plasmas in axisymmetric flow fields, AIAA Paper 85-1533, AIAA 18th Fluid Dynamics and Plasmadynamics and Lasers Conf., Cincinnati, Ohio.
- Griem, H. R. (1964). *Plasma Spectroscopy*, McGraw-Hill, New York.
- Holt, E. H. and Haskell, R. E. (1965). *Foundations of Plasma Dynamics*, Macmillan, New York.
- Jackson, J. P. and Nielsen, P. E. (1974). Role of radiative transport in the propagation of laser supported combustion waves, *AIAA J.*, 12: 1498.
- Jeng, S. M. (1986). Unpublished calculation.
- Jeng, S. M. and Keefer, D. R. (1986). Theoretical investigation of laser-sustained argon plasmas, *J. Appl. Phys.*, 60: 2272.
- Jeng, S. M. and Keefer, D. (1987a). Numerical study of laser-sustained hydrogen plasmas in a forced convective flow, *J. of Power and Propulsion*, 3: 255.
- Jeng, S. M. and Keefer, D. R. (1987b). A theoretical investigation of laser-sustained plasma thruster, AIAA Paper 87-0383, AIAA 25th Aerospace Sciences Meeting, Reno, Nevada.
- Jeng, S. M., Keefer, D., Welle, R., and Peters, C. (1987). Laser-sustained plasmas in a forced convective argon flow. Part II: Comparison of numerical model with experiment, *AIAA J.*, 25: 1224–1230.

- Jones, L. W. and Keefer, D. R. (1982). NASA's laser-propulsion project, *Aeronautics and Astronautics*, 10: 66.
- Kantrowitz, A. R. (1971). The relevance of space, *Astronautics and Aeronautics*, 9: 34.
- Karzas, W. J. and Latter, R. (1961). Electron radiative transitions in a Coulomb field, *Astrophys. J., Suppl. Series* 6: 167.
- Keefer, D. R., Henriksen, B. B., and Braerman, W. F. (1975). Experimental study of a stationary laser-sustained air plasma, *J. Appl. Phys.*, 46: 1080.
- Keefer, D., Elkins, R., Peters, C., and Jones, L. (1984). Laser thermal propulsion, *Orbit-Raising and Maneuvering Propulsion: Research Status and Needs*, AIAA Progress in Astronautics and Aeronautics series, Vol. 89 (L. H. Caveny, ed.), AIAA, Washington, D.C., p. 129.
- Keefer, D., Peters, C., and Crowder, H. (1985). A re-examination of the laser-supported combustion wave, *AIAA J.*, 23: 1208.
- Keefer, D., Welle, R., and Peters, C. (1986). Power absorption in laser-sustained argon plasmas, *AIAA J.*, 24: 1663.
- Keefer, D., Jeng, S. M., and Welle, R. (1987). Laser thermal propulsion using laser sustained plasmas, *Acta Astronautica*, 15: 367.
- Kemp, N. H. and Root, R. G. (1979). Analytical study of laser-supported combustion waves in hydrogen, *J. Energy*, 3: 40.
- Klosterman, E. L. and Byron, S. R. (1974). Measurement of subsonic laser absorption wave propagation characteristics at 10.6 μm , *J. Appl. Phys.*, 45: 4751.
- Kozlov, G. I. and Selezneva, I. K. (1978). Numerical study of a laser spark and a continuous optical discharge in a focused laser beam, *Sov. Phys. Tech. Phys.*, 23: 227.
- Kozlov, G. I., Kuznetsov, V. A., and Masyukov, V. A. (1974). Radiative losses from an argon plasma and a radiation model of a continuous optical discharge, *Sov. Phys. JETP*, 39: 463.
- Kozlov, G. I., Kuznetsov, V. A., and Masyukov, V. A. (1979). Sustained optical discharges in molecular gases, *Sov. Phys. Tech. Phys.*, 49: 1283.
- Krier, H., Mazumder, J., Rockstroh, T. J., Bender, T. D., and Glumb, R. J. (1986). Studies of CW laser gas heating by sustained plasmas in flowing argon, *AIAA J.*, 24: 1656.
- Maker, P. D., Terhune, R. W., and Savage, C. M. (1963). Optical third harmonic generation, *3rd Internat. Conf. on Quant. Electron.*, Paris, France.
- Merkle, C. L. (1984). Prediction of the flowfield in laser propulsion devices, *AIAA J.*, 22: 1101.
- Merkle, C. L., Molvik, G. A., and Shaw, E. J. (1985). Numerical solution of strong radiation gasdynamic interactions in a hydrogen-seedant mixture, AIAA Paper 85-1554, AIAA 18th Fluid Dynamics and Plasmadynamics and Lasers Conf., Cincinnati, Ohio.
- Minovitch, M. A. (1972). Reactorless nuclear propulsion —The laser rocket, AIAA Paper 72-1095, AIAA/SAE 8th Joint Propulsion Specialist Conf., New Orleans, La.
- Molvik, G.A., Choi, D., and Merkle, C. L. (1985). A two-dimensional analysis of laser heat addition in a constant absorptivity gas, *AIAA J.*, 23: 1053.

- Moody, C. D. (1975). Maintenance of a gas breakdown in argon using 10.6- μ CW radiation, *J. Appl. Phys.*, 46: 2475.
- Muller, S. and Uhlenbusch, J. (1982). Theoretical model for a continuous optical discharge, *Physica*, 112C: 259.
- Raizer, Y. P. (1965). Heating of a gas by a powerful light pulse, *Sov. Phys. JETP*, 21: 1009.
- Raizer, Y. P. (1970). Subsonic propagation of a light spark and threshold conditions for the maintenance of plasma by radiation, *Sov. Phys. JETP*, 31: 1148.
- Raizer, Y. P. (1980). Optical discharges, *Sov. Phys. Usp.*, 23: 789.
- Shkarofsky, I. P., Johnston, T. W., and Bachynski, M. P. (1966). *The Particle Kinetics of Plasmas*, Addison-Wesley, Mass.
- Thompson, R. W., Manista, E. J., and Alger, D. L. (1978). Preliminary results on the conversion of laser energy into electricity, *Appl. Phys. Lett.*, 32: 610.
- Welle, R., Keefer, D. R., and Peters, C. (1987). Energy conversion efficiency in high-flow laser-sustained argon plasmas, *AIAA J.*, 25: 1093.
- Zel'dovich, Y. B. and Raizer, Y. P. (1965). Cascade ionization of a gas by a light pulse, *Sov. Phys. JETP*, 20: 772.